LOW VOLTAGE DC TO DC CONVERTER-REGULATOR
WITH MINIMUM EXTERNAL MAGNETIC FIELD DISTURBANCE

FINAL REPORT

Contract Number NAS 5-3899

National Aeronautics and Space Administration

Final Progress Report

1 June 1954 to 30 June 1965

Goddard Space Flight Center

Greenbelt, Maryland

Submitted by

Honeywell Inc.

Ordnance Division

Hopkins, Minnesota

Honeywell

ORDNANCE

A DIVISION OF THE
MILITARY PRODUCTS GROUP

LOW VOLTAGE DC TO DC CONVERTER-REGULATOR

WITH MINIMUM EXTERNAL MAGNETIC FIELD DISTURBANCE
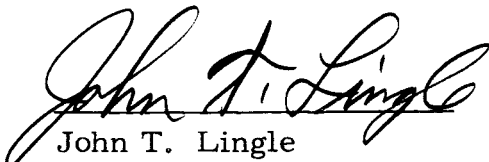
FINAL REPORT
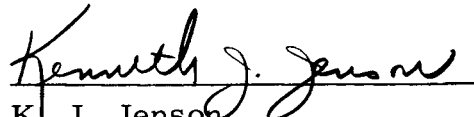
Contract Number NAS 5-3899

National Aeronautics and Space Administration

1 June 1964 to 30 June 1965
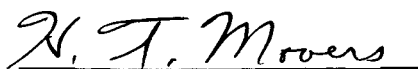
The Objective of this contract is to design and develop a low voltage dc to high voltage dc converter-regulator with minimum external magnetic field disturbance. This device will efficiently convert the inherently low voltages of newly-developed energy sources to useful higher regulated voltages and provide more reliable power systems for space applications which also have a requirement for minimum external magnetic field disturbance.

Prepared by:

John T. Lingle
Project Engineer

K. J. Jenson
Development Engineer

Approved by:

H. T. Mooers
Project Supervisor

D. I. Hinz
Section Chief

Submitted by
Honeywell Inc.
ORDNANCE DIVISION
Hopkins, Minnesota

TABLE OF CONTENTS

TABLE OF CONTENTS (Cont.)

LIST OF ILLUSTRATIONS

SECTION I
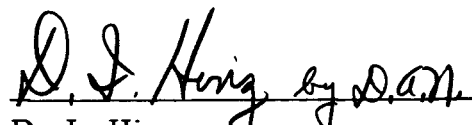
PURPOSE

The purpose of this contract was to design and to develop an efficient, reliable, and lightweight, transistor low voltage dc to high voltage dc converter with minimum external magnetic field disturbance for space applications. The converter was designed to convert the output of fuel cells, thermionic diodes, thermoelectric generators, solar cells, and high performance single cell electrochemical batteries to a regulated 28 volt dc output.

The program included circuit optimization and new design efforts to reduce external magnetic field disturbance, size, and weight. Effort has been directed toward construction of a model and magnetic field measurements to verify that the design has been optimized.

SECTION II

SUMMARY

During this program, effort was directed towards the analytical analysis of the magnetic field disturbance around the low input voltage converter-regulator (LIVCR) and towards the design, fabrication, and test of a LIVCR (Model No. EXG2424N1X1) having minimum size, weight, and external magnetic field disturbance.

Magnetic field disturbance calculations showed that a coaxial low input voltage converter design was necessary to minimize the external magnetic field disturbance which would otherwise be caused by the very high input currents (50-83 amperes). The calculations also disclosed that the output choke coil presented severe magnetic disturbance problems.

Tests verify that the coaxial low voltage converter minimizes the external magnetic field disturbance.

Since calculations indicated that a conventional choke coil would cause excessive magnetic disturbance, effort was directed toward the design and fabrication of a dual section choke coil with a totally enclosed air gap. This design, however, contained many problems including fabrication difficulties, high eddy current losses, and the need to anneal the magnetic material. Tests showed that the initial chokes fabricated had excessive magnetic disturbance. Theoretically, the design should have achieved minimum external magnetic distrubance; however, the fabrication problems would have to be solved at considerable expense before a satisfactory device could be obtained.

Successive magnetic disturbance tests were conducted on the coaxial LIVCR at Honeywell and at the Fredericksburg Magnetic Observatory,

Fredericksburg, Virginia. After each test the magnetic measurements were examined and the areas of disturbance in the unit were determined so that corrective action could be taken.

Tests showed that the magnetic disturbance from the dual section choke coil was excessive and that it became permed when operating because the mu-metal material had not been annealed after cold working. Because of this, the dual section choke design was abandoned in favor of a simple toroidal choke coil wound on a powdered 4-79 molybdenum permalloy core. Test results verified that the powdered permalloy choke produced a much lower magnetic disturbance.

The equivalent magnetic dipole of the converter-regulator was calculated from the results of the first tests at the Fredericksburg Magnetic Observatory. Subsequent measurements and calculations disclosed the magnitude and orientation of the magnetic dipoles induced by device operation. The magnitude and orientation of degaussing loops necessary to cancel these fields were calculated and inserted into the unit in convenient locations.

The last test at the Fredericksburg Magnetic Observatory was conducted with the powdered permalloy choke coil and the degaussing loops incorporated. These tests disclosed that the magnetic disturbance was greatly reduced by the incorporation of these features. Examination of the test data disclosed that the degaussing loops overcompensated the disturbance slightly. Examination of the data from the last test discloses that further modification of the degaussing loops would result in further reductions in the external magnetic disturbance. The results of the final magnetic disturbance test showed that in most instances the magnetic disturbance was within the magnetic field restraints for IMP's F and G.

Circuit investigations have resulted in several improvements which have improved the reliability, efficiency, and temperature stability of the device. The current feedback power oscillator circuit has been improved by the incorporation of circuitry which provides higher back bias voltages to switch the oscillator transistors much more rapidly. This feature speeds the power oscillator switching, reduces switching losses, and allows operation at higher frequencies which result in weight reduction. The pulse width modulation voltage regulator has been improved by the use of current drive to forward bias the power chopping transistor and a snap acting back bias circuit to provide a more effective back bias arrangement. These features maintain higher voltage regulator efficiency throughout wide load and input voltage ranges and provides adequate drive during overlaod operation.

The low voltage converter-regulator was designed to have an efficiency above 75% at 50 watts load when operating from inputs between 0.8 and 1.6 vdc. Tests show that the converter-regulator exceeds these efficiency requirements for all input voltages except the 1.6 volt value where the efficiency is 73.5%. An efficiency exceeding 75% can be achieved at this 1.6-volt input if internal connections inside the regulator package are made for a higher input voltage range of (1.2 to 1.8 volts). These transformer tap connections are not readily accessible unless the regulator section is disassembled. Because of this, the unit has been shipped with connections made for the 0.8- to 1.6-volt range.

The performance of this converter-regulator was checked at -10°C, 25°C, and 70°C and was found to perform satisfactorily. The efficiency increases about 3% at -10°C and decreases about 3% at 70°C. The device overload current limiting circuit is suitable for battery charging and protects the device from slowly increasing overloads as well as sudden dead shorts.

Further effort should be devoted to weight reduction. This 50 watt low voltage converter-regulator weighs 5.16 pounds. The incorporation of the powdered permalloy choke coil to reduce the magnetic disturbance resulted in a 3/8-inch increase in length and raised the weight from 4.8 to 5.16 pounds. The volume of the device is less than 90 cubic inches.

SECTION III

CONFERENCES

During the final quarter two informal meetings were held. Mr. J. T. Lingle from the Honeywell Ordnance Division met Mr. E. Pasciutti from the National Aeronautics and Space Administration - Goddard Space Flight Center, at the Nineteenth Annual Power Sources Conference on May 19, 1965 and discussed technical details of this program. On 3 and 4 June 1965, Mr. J. T. Lingle and Mr. K. J. Jenson from Honeywell conducted magnetic disturbance tests at the Fredericksburg Magnetic Observatory with the assistance of Mr. R. Kuberry, the Observer-in-Charge.

On 3 June, 1965 Mr. Pasciutti visited the test site and witnessed the magnetic disturbance tests. Technical discussions were held regarding the magnetic distrubance measurements and the magnetic disturbance requirements for spacecraft. Because these tests showed that the magnetic disturbance at the regulator end of the device was excessive, Mr. Pasciutti suggested that further efforts should be made to reduce the magnetic disturbance in this area. He also observed that the long length of the converter-regulator caused the end of the converter containing the disturbance to come within nine inches of the sensor when the device was rotated about its geometric axis. In this position the reduction in distance amplified the disturbance by a factor of eight. Mr. Pasciutti stated that the test results would be more meaningful if the measurements were made at a greater distance because the device shape would have less effect. In this regard, Mr. Pasciutti re-examined the magnetic requirements and stated that to make a reasonable comparison between our magnetic test data and actual space craft requirements we should compare our results with a recent NASA-Goddard Space Flight Center document "Magnetic Field Restraints for IMPS F and G" by N. F. Ness.

After examination of the data obtained on 3 and 4 June, the regulator section was reworked and a second magnetic disturbance test was conducted at the Fredericksburg Magnetic Observatory on 24 and 25 June 1965. These tests showed considerable improvement and the tests results are discussed in detail in the report and compared with the NASA-Goddard Document.

SECTION IV

PROJECT DETAILS

A.   COAXIAL DESIGN

In the performance of this contract, the low input voltage converter-
regulator (LIVCR) with minimum external magnetic disturbance was
studied, designed, and fabricated. It was initially determined that
coaxial construction and a coaxial input lead were necessary to minimize
magnetic disturbance due to the very high dc currents carried by the low
voltage section. It was also determined that the concentricity of the coaxial
conductors should be held to 0. 002 inch in order to limit the magnetic dis-
turbance to acceptable levels.

Transformers and inductors have been designed utilizing toroidal construc-
tion and high permeability core materials in order to achieve very low ex-
ternal magnetic disturbance.

The coaxially constructed converter is shown on Figure 1 of this report.
Construction details are described in Progress Report 2 and more clearly
in Figures 1, 2, and 3 of that Report. The concentric coaxial con-
struction minimizes the external magnetic disturbance because each
conductor produces an equal and opposite magnetic field. This results in
total cancellation of the net fields due to the very high input current.
This problem is quite severe in the case of low voltage converters because
of the very high input currents. The coaxial construction has been used
throughout the high current primary circuit including the input lead, bus
work, and power transformer primary. Transformers and inductors have
been designed utilizing toroidal construction and high permeability core
materials in order to achieve very low external magnetic disturbance. The
construction details of this device are thoroughly described in Progress
Report 2.
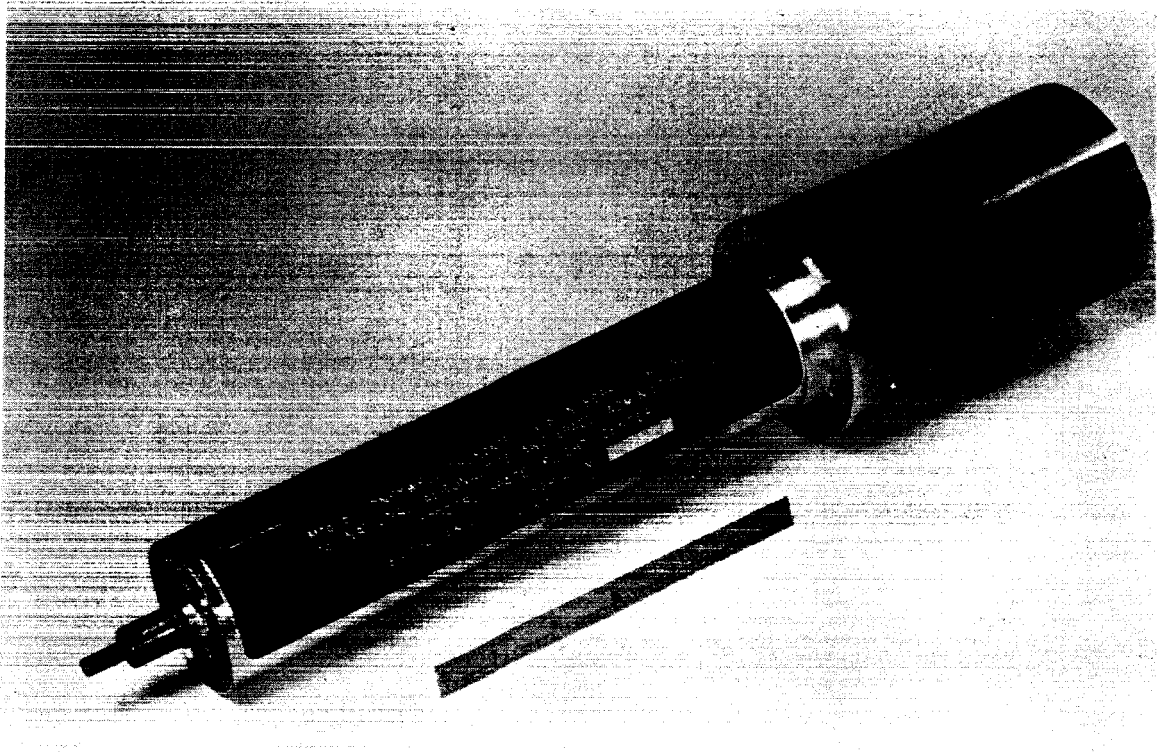
Figure 1 - PHOTOGRAPH OF COAXIAL LIVCR EXG 2424N1X1

Besides minimizing the external magnetic disturbance, the coaxial construction has also provided the following features:

1. Minimizes the inductance of the input lead and primary circuit (this diminishes voltage spikes at the converter input during switching, and tends to improve over-all efficiency as will be discussed later).

2. Heat transfer requirements in this coaxial low input voltage converter design were carefully considered. The germanium power oscillator transistors are located inside the package near the ends. A large cross sectional area short thermal path has been provided from the transistor cases to the outer shell of the low input voltage converter regulator. Thus, temperature rise in the transistors is minimized because the heat can readily flow from the collector through the excellent thermal path to the outer case of the converter section where it can be readily transferred to the ambient by conduction, convection or radiation.

B. CIRCUIT DESCRIPTION

The low input voltage converter regulator is shown in Figure 2 (block diagram) and Figure 3 (circuit diagram). A current feedback power oscillator chops the low voltage high current to square wave and transforms it to a higher, more usable voltage. A starting oscillator guarantees starting under all environmental conditions and a voltage regulator achieves regulation by pulse width modulation. An output current limiting circuit is included for overload protection. The output filter smooths the pulse modulated dc to provide the regulated and filtered dc output.

1. Low Input Voltage Converter

The low input voltage converter section (Figure 3) consists of a push pull power oscillator stage composed of transistors Q1, Q2, A3, Q4, current feedback transformer T1, pulse transformers T3 and T4, and power transformer T5. Current feedback drive proportional to load is provided by transformer T1 to operate transistors Q1, Q2, A3, and Q4. The oscillator operating frequency is controlled by saturable reactor L1, which couples negative feedback from winding N3 on power transformer T5 and to winding N3 on current feedback transformer T1. When reactor L1 saturates at the end of each half cycle, negative feedback from the power transformer overrides inherent positive feedback in the current transformer T1 to recycle the circuit. Small pulse transformers T3 and T4 improve the power oscillator switching characteristics. These effectively decouple the switching off transistor from the feedback transformer T1 windings, so that the switching off transistor can be momentarily back biased to a much higher voltage during switching. Normally, the emitter base voltage of the conducting transistor acts like a zener diode clamp and tends to maintain the induced voltage on the T1 windings at a constant value. This establishes a maximum voltage of approximately 0. 45 volts on windings N2A and N2B on T1, and normally limits the maximum back biased voltage applied to the switching off transistor to the forward V_{BE} (SAT.) value of
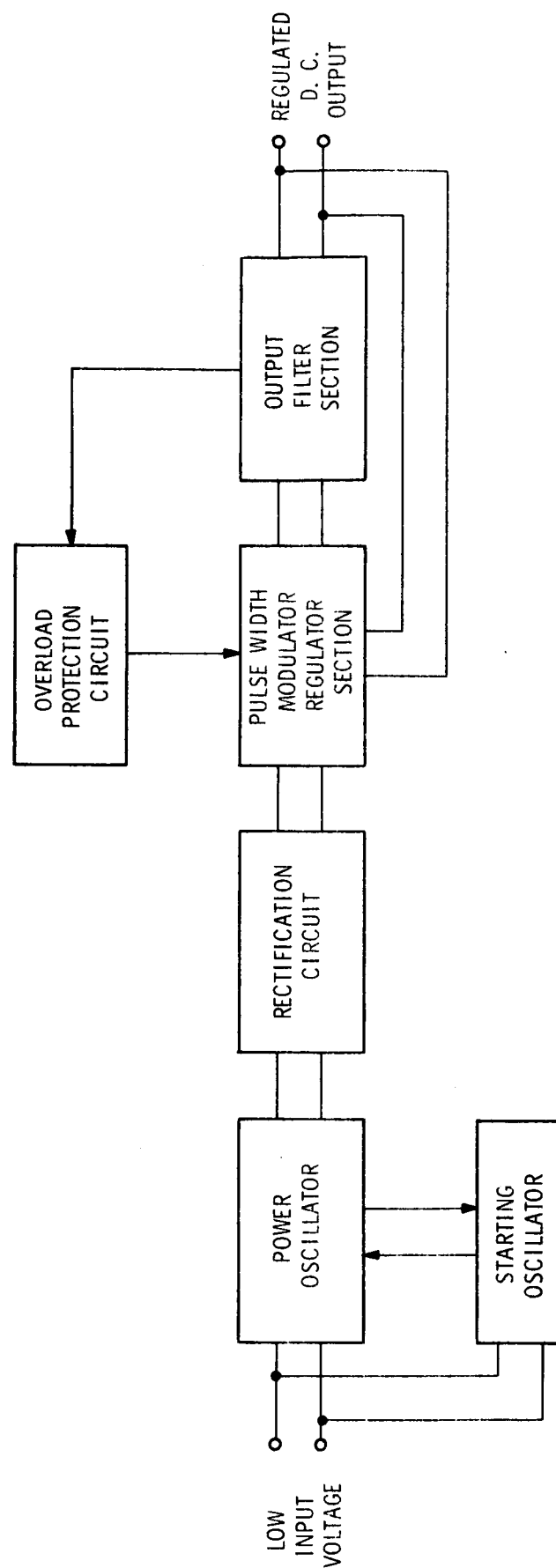
Figure 2 - BLOCK DIAGRAM OF THE LIVCR
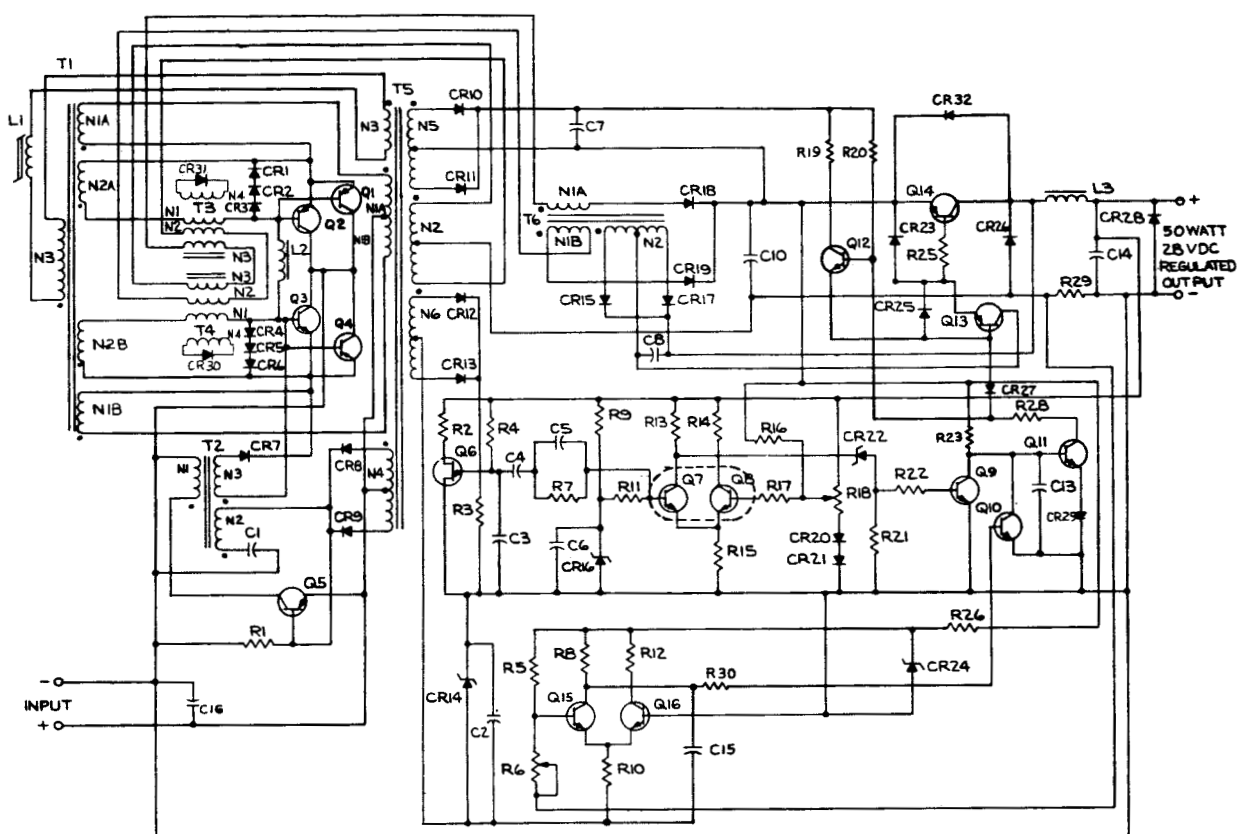
Figure 3 - LIVCR EXG 2424N1X1 CIRCUIT DIAGRAM

0. 45 volts. When pulse transformers T3 and T4 are incorporated into the circuit, they momentarily decouple transformer winding N2 from the switching off transistor, remove the effective voltage clamp, and allow the switching off transistor to be back biased to a much higher voltage. This momentary high back biased voltage sweeps the stored carriers out of the base region more rapidly so that the power oscillator is switched rapidly. This feature reduces the power oscillator switching losses, provides higher efficiency, and allows the device to be operated at higher frequencies where considerable weight reduction can be realized. Positive feedback from either transformer T3 or T4 and the resetting of reactor L2 provide the momentary higher back biased voltage which turns the switching off transistors off much more rapidly. Reactor L2 also draws current out of the bases of the switching on transistors and this tends to provide an initial overdrive to switch these transistors on rapidly.

This power oscillator is normally self starting. However, a starting oscillator consisting of transformer T2, transistor Q5, diodes CR7, CR8, CR9, capacitor C1, and resistor R1 is provided. The starting oscillator applies a pulse to the base emitter junction of transistors Q3, Q4 through diode CR7 to guarantee starting of the converter under all environmental conditions. A bias voltage from winding N4 on transformer T5 and diodes CR8 and CR9 is applied to the starting oscillator once the main power oscillator has initiated. This bias voltage shuts off the starting oscillator and renders it inoperative, after the main power oscillator starts.

2.   Voltage Regulator

The pulse width modulation voltage regulator has very low losses and maintains high efficiency over the wide input voltage and load ranges. Capacitor C10, between the converter output and the regulator input, prevents the regulator pulse modulation effect from being fed back into

source and the emitter based junction of the chopping transistor. The back bias power is obtained from transformer T5 winding N5 through rectifiers CR10, CR11, and capacitor C7. The snap acting gate circuit which controls the back bias consists of resistor R19, R20, transistor Q12, and diode CR27. When the pulse forming circuitry switches transistors Q11, Q13, and Q14 on, current flows through diode CR27. The forward voltage drop across this diode back biases transistor Q12, rendering it non-conductive and removing the back bias power flow to transistors Q13 and Q14.

Conversely, when transistors Q11, Q13, and Q14 are switched off, current flow through diode CR27 is removed and and a positive bias is applied through resistor R20 to the base of transistor Q12. This renders transistor Q12 conductive and back bias current flows through R19, Q12, into the bases of transistors Q13 and Q14, shutting them off rapidly. The higher power available from the low impedance source C7 through the low impedance of conducting transistor Q12, switches Q14 off more rapidly to reduce the turn-off losses. The resultant higher back biased current removes the stored carriers from the bases of Q13 and Q14 quickly to accomplish rapid switching. This snap acting circuit also removes the back bias signal from transistors Q13 and Q14 when they are gated into conduction. This diminishes the amount of current that transitor Q11 must switch because it no longer has to handle both the forward drive and the back bias drive requirements simultaneously. This feature increases the voltage regulator gain.

3.   Overload Current Limiting

The load current through a very small resistor R29 is sensed by a differential detector consisting of transistors Q15 and Q16. This circuit is biased by resistors R5, R6, and R29 so that transistor Q15 is normally conducting more than Q16. Resistor R6 is adjusted to control the overload current set point. During overload the voltage drop across resistor R29 increases

to a value which causes the base of transistor Q16 to become more positive than the base of transistor Q15, and Q16 begins to conduct more heavily at the pre-set load current level. This diminishes the conduction of Q15 and applies a positive voltage to the base of transistor Q10.

When transistor Q10 conducts, it back biases transistor Q11 and shuts off the pulse width modulator. The circuit has very fast response and rapidly shuts off the pulse width modulator during overload and thus protects the converter and output circuit from excessive load currents. This current limiting circuit will maintain the output current at the pre-set overload current level during overload and short circuit conditions. This characteristic allows the circuit to be used very effectively for battery charging applications and the powering of dc motors which may draw initial overloads when starting or accelerating. The circuit functions for either slowly increasing overloads or sudden dead shorts. It recovers immediately when the overload is removed. Experiments have shown that when transistors Q15 and Q16 are incorporated into a common can, the temperature stability of the circuit is improved.

C.   CIRCUIT IMPROVEMENTS

The improvements which ave been incorporated into the low input voltage converter regulator circuit during this program are as follows:

1.   Improved current feedback power oscillator which back biases the switching off transistors to a higher voltage to accomplish more rapid power oscillator switching.

2.   Current drive for the voltage regulator pulse modulating transistors.

3.   A snap acting gate circuit to back bias the pulse modulating transistor.

4.   Simplification of the voltage regulator circuit and the starting
        oscillator.

5.   Modification of transformer core hysteresis loop to diminish
        effects of effective dc components.

The improved current feedback power oscillator section provides more rapid
switching of the low saturation voltage high current transistors. This reduces
switching losses, improves efficiency, allows the device to be operated at
higher frequencies where weight reduction of the unit can be achieved. The
current drive for the voltage regulator chopping transistor provides a more
optimum drive which reduces losses over the wide input voltage and load
range. It also guarantees that the chopping transistor will operate safely in
the low saturation region during the heavy overload conditions. In the previous
units, voltage drive was used and it was necessary to provide drive for the
worst case conditions (heavy load and low input voltage). This resulted in
excessive drive under the other conditions. Also it did not provide sufficient
drive during overload, and as a result the circuit was more marginal
under overload. The snap acting back bias circuit has allowed the back
bias power drain to be reduced in a voltage regulator and has provided
more rapid switching because the drive transistor does not have to switch
the back bias power as well as the forward bias signal. The incorporation
of the improved back bias circuit has provided better temperature stability,
higher circuit gain, and higher switching efficiency for the pulse width
modulation voltage regulator.

Modification of the transformer core hysteresis loop has been accomplished
by placing an air gap in a portion of the magnetic circuit. This air gap
is introduced in approximately 30% of the core cross sectional area and it
diminishes the tendency of a small effective dc unbalance current from
saturating the transformer core toward the end of one half cycle. If the air
gap is not included, an effective dc component will operate the core off the

hysteresis loop center and the core can saturate just before the end of one half cycle. When this occurs, the transformer magnetizing current and transistor collector currents rise to a very high value. This tends to increase the switching losses because the current voltage product becomes very high during switching. Also the high current increases the energy stored in the input lead and primary inductance and this produces an input voltage spike during switching which further increases switching losses. The high transistor collector current during switching also increases the switching time resulting in a further increase in switching losses. Thus operation of the transformer in a mode which allows saturation toward the end of one half cycle causes cumulative effects which increase the transistor switching losses.

The incorporation of a partial air gap in the magnetic circuit has greatly diminished this effect and has resulted in higher efficiencies.

D.   STRESS ANALYSIS

A circuit stress analysis was conducted and parameter variation calculations were programmed on a computer. These studies disclosed that changes in the values of some components were necessary to operate the components conservatively within their ratings. These changes have been incorporated in the 50 watt model.

E.   SELECTION OF COMPONENTS AND MATERIALS

Minimum magnetic disturbance criteria were used for the selection of components and materials. High permeability narrow hysteresis loop materials such as supermalloy, 4-79 Molybdenum Permalloy, and mu-metal have been used for the magnetic cores. For the most part aluminum electrolytic capacitors have been used because of their non magnetic construction.

-19-

Small solid tantalum capacitors have been used in some locations and the leads have been trimmed very short to minimize disturbance by reducing the magnetic material mass. Transistors with non magnetic cases available were purchased for use in this unit. Four Honeywell MHT 2202 transistors were used in the power oscillator. These were basically non-magnetic except for the copper cored kovar base lead which was trimmed to a minimum length. Some special 2N2833 transistors with a non-magnetic cover were purchased for use as the voltage regulator chopping transistor. Measurements, however, showed that the 2N2833 units with non-magnetic covers produced greater disturbance than the standard units with steel covers.

The greater disturbance was probably caused by nickel plating on the unit with non-magnetic covers. A standard 2N2833 transistor was used in the fabrication of the model because it produced less magnetic disturbance than the special 2N2833 units purchased for this purpose. Some small signal transistors with non-magnetic cases were also obtained. However, they did not meet the electrical parameter requirements and hence were not used in the model. The small signal transistors used had magnetic cans and magnetic leads because non-magnetic units could not be obtained at reasonable cost. Preliminary tests showed that these small signal transistors create an appreciable disturbance even though the magnetic mass of the devices used in the regulator is relatively small.

F.   CHOKE COIL DESIGN

1.   Dual Section Choke Coil

The fabrication of the dual section laminated core choke coil with internal air gaps and with the desired magnetic properties has involved some difficulties. Some of these difficulties were discussed in Progress Report 3 in conjunction with the first fabrication of a choke coil of this type.

One of the major problems encountered in that first model was the high eddy current losses in the core, due to inadequate insulation between the laminations. Recognizing this problem, core material with an "insulaze" coating was used in fabricating the second model. During the fabrication of the second model, however, it was found that the "insulaze" coating was inadequate for two reasons. First, the coating was so thin that the rubbing together of any two laminations during fabrication wore the coating through so that the laminations were electrically shorted together. Secondly, it was found that the burrs created while cutting the laminations to size lapped over between laminations negating any residual insulation which may have been present. This tended to occur even when the cut surfaces were ground. The end result was that no effective lamination insulation was realized. This absence of insulation once again resulted in high eddy current losses.

A third model was fabricated incorporating a 0.5 mil thickness of Mylar between laminations in addition to the insulaze coating for the center core section and the outside wraps. The end bell laminations were cemented together with lamination cement which provided an insulated coating in addition to the insulaze. These techniques proved to provide effective insulation between laminations and reduced eddy current losses considerably.

A more specific understanding of the fabrication of this third model can be had from referring to Figure 4. The geometry of the core differs from that model discussed in Progress Report 3 only in the end bells. Each end bell (A_1, A_2, A_3, A_4) for this third model consisted of four orthogonal laminated sections held in position with a nylon form (Figure 5). The individual laminations in each section were fabricated from 14 mil mu-metal to reduce the number of necessary laminations and facilitate fabrication. When cut and machined to size, each laminated section was
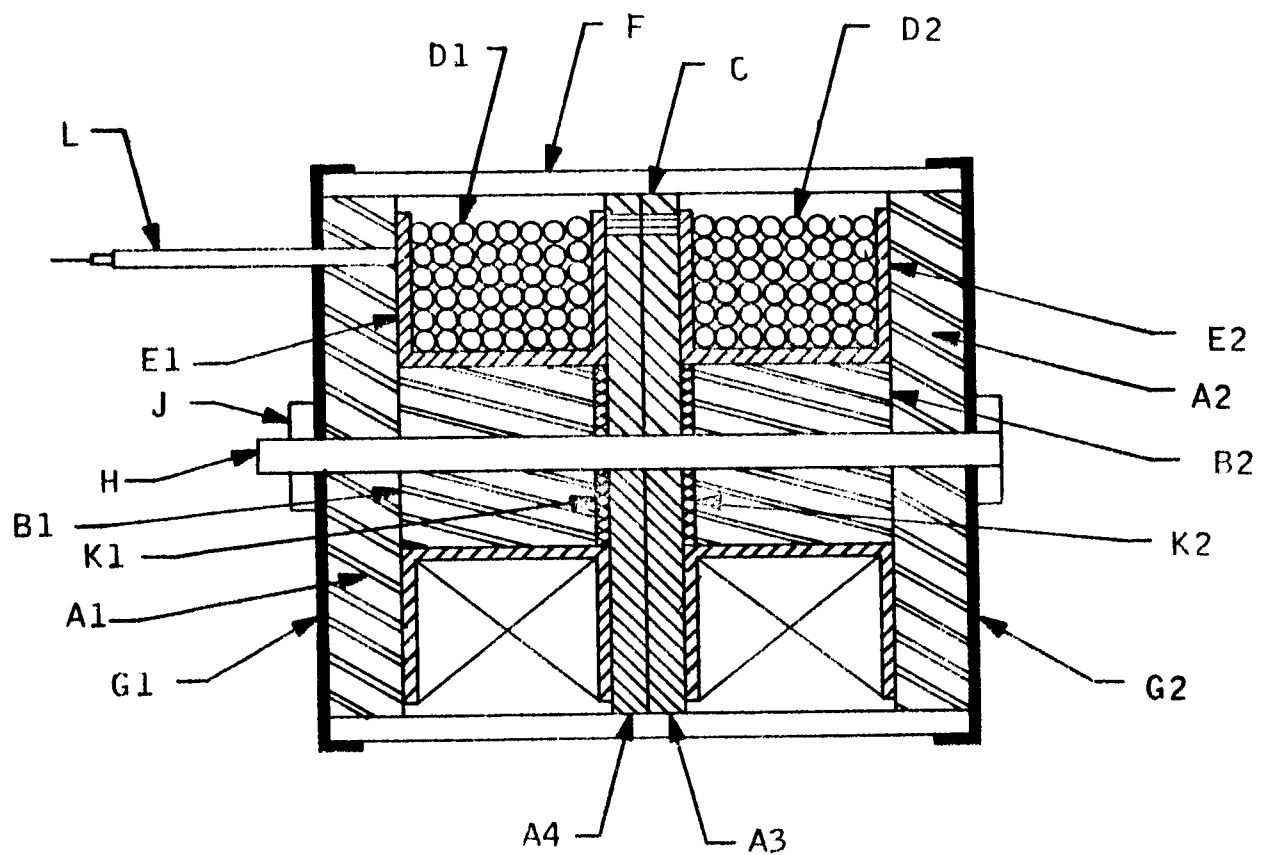
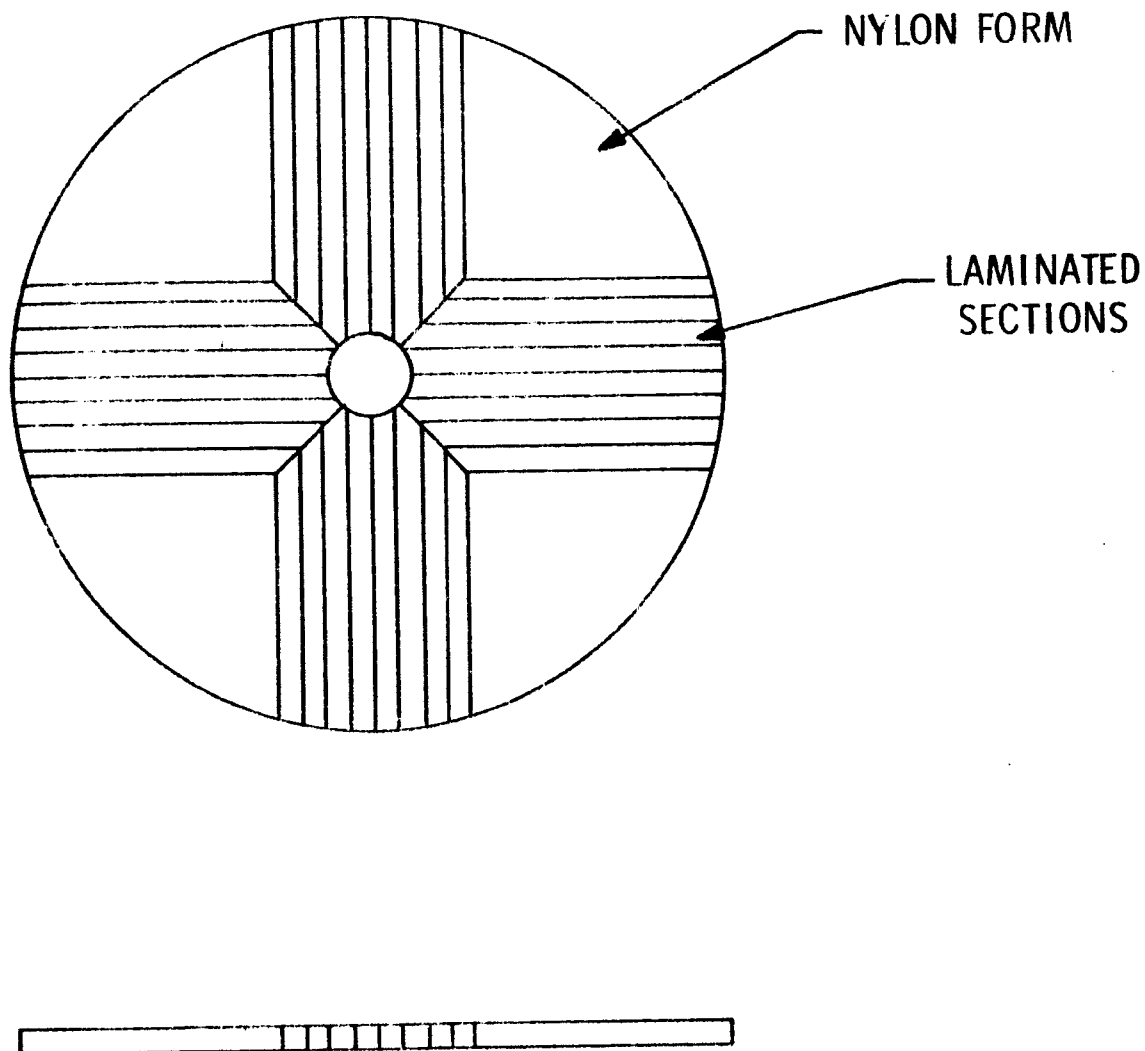Figure 4 — DUAL CHOKE COIL CONSTRUCTION

NYLON FORM

LAMINATED
SECTIONS

Figure 5 - END BELL CONSTRUCTION FOR DUAL CHOKE COIL

-23-

cemented together under a vacuum to obtain a more uniform and complete coating of each lamination. The central part of the core (B1, B2) was fabricated by wrapping 6 mil mu-metal around a mandrel and building up a laminated spiral core. The fabrication procedure for this central section consisted of:

1. Winding the material on a mandrel.

2. Machine this to the proper length.

3. Unwinding the material.

4. Re-winding the material on a mandrel with a layer of Mylar wrapped as an inter-winding insulator.

5. Trimming the Mylar extending beyond the machined surface by burning it off.

The coils D_1, D_2 for each section were wound upon two bobbins E_1, E_2. The ends of D_1 and D_2 respectively are common and their beginnings are terminated inside the case in respective wires, which are coaxial with each other. Over this assembly a strip of mu-metal with a Mylar insulator is wrapped to form the outer cylindrical case F.

Some core air gaps were created during fabrication at the central core - end bell junctions and the end bell - outside wrap junctions. These gaps were a result of the tradeoffs of maintaining very small core gaps and still realizing lamination insulation. To avoid shorting the laminations together, it was found that more effective gap than is desirable had to be allowed. This gap may be decreased if more time and funds were available to perfect the fabrication procedure. The leakage flux emanating from these gaps, of course, is undesirable.

This total assembly is enclosed by, but insulated from a mu-metal shield.

A stainless steel screw H passing through the center cores and the end bells with nuts J on each end, hold the entire shielded choke assembly together and provides a stud mounting for the assembly.

The fabricated choke assembly had three significant undesirable features. Namely: (1) a distributed air gap (as discussed above) due to the fabrication procedure necessary to realize laminar construction, (2) deviation in the magnetic properties (from the annealed) due to cold working, and (3) increased weight as compared to other choke coil designs.

The change in magnetic properties because of the cold working proved to be a major problem because the change reduced the theoretical inductance of the choke and also caused the material to retain a high degree of magnetism after exposure to a strong magnetic field. The material was not annealed after choke fabrication because the high temperatures necessary for annealing would remove the interlaminar insulation and the insulation from the copper wires encased by magnetic material. (These wires had to be incorporated during the fabrication process.) The high cost and involved procedure to anneal and yet retain laminar insulation in this unconventional, one-of-a-kind construction also proved to be a limiting problem.

Magnetic disturbance testing verified that annealing of the materials would be necessary for incorporation into a low external magnetic disturbance device. Although more extensive efforts could result in a solution to the annealing problem, none was found during work on this contract.

The dual section laminated core choke coil weighed approximately twice as much as the comparable choke and choke.

2.   Magnetically Shielded "C"-Core Choke Coil

A conventional "C"-Core type choke coil was fabricated and magnetically shielded with Shield mu-30 alloy to provide an alternate to the dual internal air gap, laminate choke coil approach. Both approaches reduce the external magnetic radiation from an air gapped core. The internal air gap approach is the most sophisticated because it attempts to both minimize the generation of a dipole and to reduce flux fringing by keeping the air gap internal to the actual core material. The shielded "C" Core approach merely shunts the air gap leakage flux before it reaches the external surroundings. Fabrication difficulties have made it impossible to realize the ideal magnetic properties desired in the internal air gap, laminar choke coil and thus the shielded "C" core type was fabricated. The shielded "C" core provides an alternative and also a basis for comparing the magnitude of radiated flux.

The choke coil itself is of the conventional "C" core type construction. The magnetic shielding of it consisted of two Shield mu-30 cans magnetically insulated from each other and the choke coil. The total shielded assembly weighs 0.5 pounds and occupies a volume of 7 cubic inches.

The coil commutates very well over the input voltage and load range.

The problems in annealing the mu-metal in the dual section choke were also present to a lesser degree in annealing the "C"-core shield. It would be possible to anneal the shield when disassembled and then assembling the shield around the choke with minimum post anneal working of the material. This procedure would eliminate the necessity of exposing the choke coils to the high annealing temperatures. Some special fixtures would be necessary, however, to anneal the shield and yet retain laminar insulation. Because the "C"-core (Silectron) itself had a high residual flux density, it was felt that this special fixturing necessary for annealing was not worth the time and effort. The disturbance testing indicated that the silectron and cold worked shield did retain a high degree of magnetism.

-26-

3.   Powdered Permalloy Choke Coil

The output choke coil used in the final design of EXG2424N1X1 utilized a 4-79 powdered permalloy toroidal core. The windings were evenly distributed about this core to reduce its magnetic disturbance due to circulating currents. This coil displayed a high inductance commutating well over the input voltage and load range. The testing at the Honeywell Laboratory and the Fredericksburg Observatory showed that the magnetic disturbance of this choke was much less than had been obtained with previous chokes. The actual disturbance effected is considered in conjunction with the LIVCR disturbance testing at the Fredericksburg. Observatory.

G.   MAGNETIC DISTURBANCE TESTS

Preliminary magnetic measurements were made at Honeywell and these disclosed that the choke coil caused considerable difficulty. Because of this, the choke coil was redesigned. Also an alternate coil consisting of a conventional "C"-core choke enclosed within a magnetic shield, was fabricated for the more exacting tests at the Fredericksburg Magnetic Observatory. Magnetic disturbance tests were then conducted on June 3 and 4, 1965, at the Fredericksburg Magnetic Observatory. These tests disclosed the following:

1.   When non-operating, the converter regulator did not appear to produce excessive disturbance, however, it was noted that the major disturbance occurred at the regulator end.

2.   When the device was rotated about its geometric center, the ends of the converter regulator came very close to the sensor and hence the magnetic disturbance was increased in the position where the end (the regulator end) was closest to the sensor.

3. When operating the coaxial input line alone with a shorted plug at the end where the converter normally connects, the line itself caused considerable magnetic disturbance. This is probably due to a lack of concentricity in the coaxial input line.

4. When the converter was operated it was noted that there was a considerable increase in the magnetic disturbance. Measurements indicated that the major disturbance occurred in the regulator end.

5. When the converter regulator was operated with the choke coil removed from the unit and connected to it by means of a very long coaxial lead, the magnetic disturbance was much less. These measurements verified that the choke coil was a major cause of magnetic disturbance.

6. The measurements also disclosed that the low input voltage converter regulator with the choke coil included, tended to pick up a perm after operating. When the choke coil was removed, this effect was greatly dimished, however, a noticeable perm was still present.

7. These tests verified that the choke coil was still a cause of considerable magnetic disturbance. Because of this additional measurements were taken of the converter regulator operating with the choke coil removed and of the choke coil operating alone.

8. Since the converter regulator still produced considerable disturbance at the regulator end with the choke coil removed, the field around one of the 2N2833 transistors was also mapped and it was found that this device had considerable disturbance.

9. The converter regulator was also de-permed and checked after de-perming, and it was found that it could be de-permed resonably satisfactorily.

10. After being subjected to the 25 gauss field it was found that the unit became permed, particularly at the regulator end. These tests showed that the transistors used in the regulator end with their can and leads made from magnetic material, produced an appreciable disturbance both when operating and after operating, because they tended to pick up a perm during operation. Since these components are located near the end of the device, the disturbance that they create becomes more noticeable as the regulator end is rotated close to a sensor.

The above tests verify that the choke coil was causing difficulty and it also showed that the transistors and other semiconductors, which had magnetic cans and magnetic leads, produced an appreciable disturbance even though their leads were trimmed to a minimum. These tests also tended to show that the low input voltage converter section appeared to have relatively low magnetic disturbance comparing favorably with the design goals. Thus, the feasibility of fabricating a low input voltage converter with minimum magnetic disturbance was proven. However, since the regulator section, and particularly the choke coil, produced excessive disturbance the tests showed that some rework of this section was desirable. The operating and non-operating measurements on the converter regulator with the choke coil removed provided us with information which allowed us to calculate the magnetic dipole of the device for both operating and non-operating

conditions. Because the magnetic disturbance of the regulator section was greater than desired, it was decided to rework this section. The test data was examined and calculations were made to determine the strength of the magnetic dipoles inherent in the unit. A new choke coil was designed utilizing 4-79 powdered permalloy toroidal cores. The windings were evenly distributed about this core and preliminary checks in Hopkins showed that the magnetic disturbance of this core was much less than had been obtained with the previous choke coils. The data taken at Fredericksburg was analyzed and the respective magnetic dipoles of the unit were determined. From this data, degaussing coils were designed to cancel out the effective magnetic dipoles. These were inserted in the unit and given further preliminary checks at Hopkins. One degaussing coil is located at the end of the regulator and cancels a field along the device axis.

The other degaussing coil is located in the regulator section transverse to the device axis near the power transistor to cancel a field which was transverse to the converter regulator axis. With these changes incorporated in the unit, further preliminary magnetic tests at Hopkins indicated that the magnetic disturbance was much lower and the unit was prepared for further tests at the Fredericksburg Magnetic Observatory.

1.   Initial Magnetic Disturbance Tests

a.   Stray Power "On" vs. Power "Off" Tests - The initial testing to determine the difference in the magnetic field, associated with power-on/ power-off conditions of the coaxial LIVCR, was conducted with the dual section choke coil mounted in the LIVCR. The maximum difference measured 18 inches from the geometric center of the LIVCR was greater than 40 gamma. The majority of this disturbance appeared to be coming from the dual section choke indicating this to be a specific problem area. To verify this, the choke coil was removed from the unit and once again tested (electrical continuity to and from the removed choke being maintained through a coaxial lead). The magnetic disturbance measured, when the choke was

removed, was greatly reduced over the previous readings. The remainder of the power on vs. power off testing was conducted with the choke coil removed to allow the isolation of any additional disturbance problem areas in the LIVCR.

Some additional testing with the dual section choke and the shielded "C" core choke isolated from the LIVCR provided a basis for an evaluation of their performance.

The testing of the LIVCR (without choke coil) determined that the difference in the magnetic field associated with power on/power off conditions can be approximated by a dipole along the LIVCR longitudinal axis, plus a dipole perpendicular to the longitudinal dipole. This testing also showed that the majority of the difference field was caused by circulating currents in the regulator section. With the regulator section producing the largest difference field, it followed that the maximum LIVCR disturbance at 18 inches from its geometric center, was noted on a line collinear with the longitudinal axis and off the regulator end of the package. It is felt that the largest contributing factors to this disturbance are those currents passing through circuit components (such as capacitors, transistors, and diodes) which cannot be effectively compensated by equal and opposite currents. The fact that the location of these effective dipoles is off the geometric center of the package results in a dipole-to-test point separation which is considerably less than the package geometric center to test point separation. The difference field measured at 36 inches from the geometric center in the worst case direction was in the neighborhood of 1 gamma. The exact difference at this distance could not be determined because of a very low signal to noise ratio for measurements of less than 1 gamma.

A mapping of the power on/power off magnetic field difference for the LIVCR operating with the output choke coil removed is presented in Figure 6. The source of this generated field can be approximated by two dipoles both of which are assumed to be located at the junction of the converter and regulator sections. One dipole is directed toward the input along the longitudinal axis of the unit with a magnitude of approximately 550×10^{-5} amp-meters^2. The other dipole is perpendicular to the longitudinal axis directed toward the output connector and 10 degrees upward (Figure 7). These dipoles are only rough approximations but they did provide valuable information for designing compensating windings for the finalized unit.

b.   Post 25 Gauss Explosive Test - The calculation of the major magnetic dipole is shown in Appendix A. After perming the converter with a 25 gauss field and evaluating the test data, it was determined that a dipole having a strength of 2.79×10^{-3} ampere meters squared existed in the regulator section directed along the longitudinal axis. This dipole is located 11.5 centimeters from the geometric center of the low input voltage converter regulator in the regulator end. The data taken on the 2N2833 transistor also showed that it had a strong dipole. This was an appreciable percentage of the total magnetic dipole of the unit. The magnetic dipoles of the several smaller transistors which are actually located nearer the end, probably make up the major portion of the remaining magnetic disturbance.

2.   Current Loop Compensation

Two current loop compensating dipoles were incorporated into the coaxial LIVCR to reduce the power on/power off magnetic field difference. These dipoles were added using (1) information obtained in the first series of tests at the Fredericksburg Magnetic Observatory with the LIVCR operating with a removed output choke coil and (2) magnetic measurements taken in
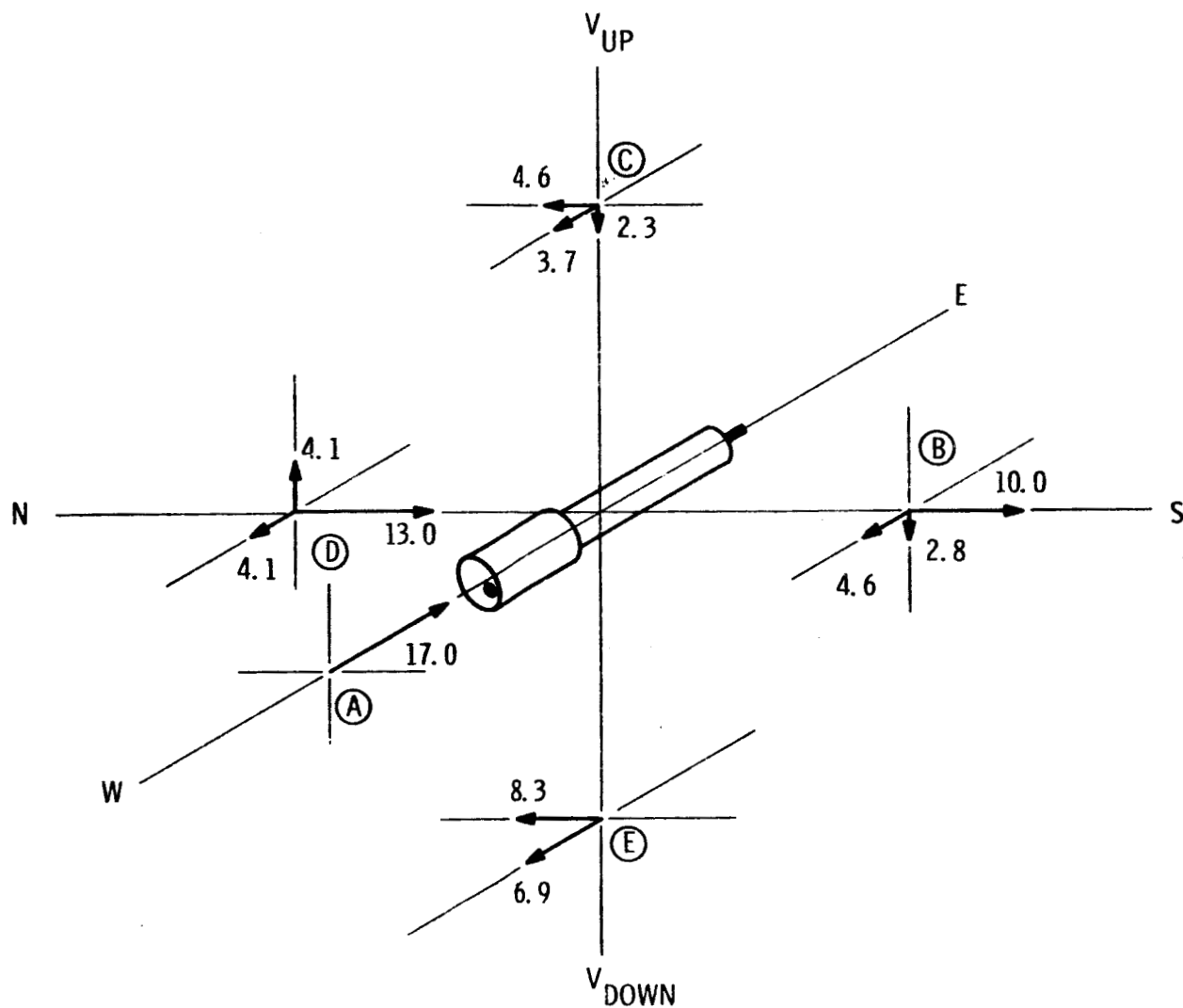
NOTE: DISTURBANCE IN GAMMA

LIVCR OPERATING AT FULL LOAD

TESTS CONDUCTED JUNE 3-4, 1965

TESTS POINTS REPRESENTED BY ENCIRCLED LETTERS.

Figure 6 - POWER ON/POWER OFF MAGNETIC FIELD DIFFERENCE FOR LIVCR OPERATING WITH A REMOVED CHOKE COIL
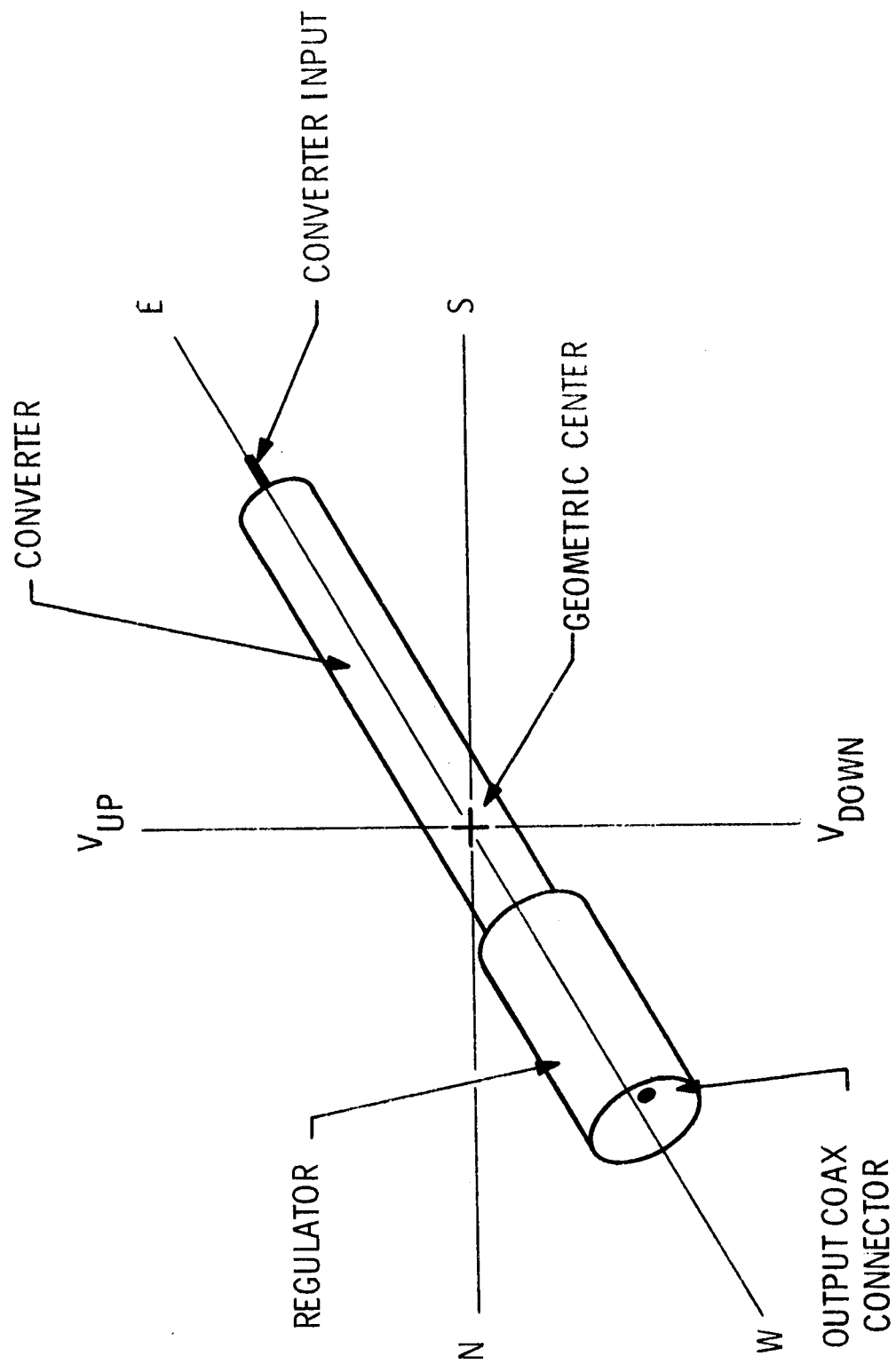
Figure 7 - ORIENTATION REFERENCE FOR LIVCR EXG 2424N1X1
MAGNETIC FIELD TESTING

Honeywell Laboratory with the LIVCR operating with the powdered permalloy core output choke incorporated. The ambient magnetic noise, the accuracy of the magnetometer available, and the inability to completely zero the earth's field proved to limit extensive testing at the Honeywell Laboratory; however, this testing did provide reasonably accurate results when compared with those at the Observatory and were a valuable design aid. The testing at the Honeywell Laboratory was especially useful in verifying that measurements made at distances up to 18 inches separation from the geometric center of the device revealed not a simple dipole representation of the LIVCR's disturbance but a rather complex and multi-dipole device. This is rather obvious when the device is given careful consideration. The device itself is approximately 15 inches in length. Small contributions to the total magnetic field of the device are made at distributed points along its entire length. While these small contributing dipoles may be resolved into one single dipole when the measuring distance is large compared with the dipole separation, this is not necessarily the case when measuring at 18 inches. It would, however, more likely be the case when measuring at 36 inches. This was noted especially in the testing in the Honeywell Laboratory when measurements were made at a separation distance of only 9 inches. This distance was first chosen so that the signal level would be larger in comparison to the noise level in the laboratory and this supposedly would make our measurements more accurate. It was found, however, that the field characteristic changed so drastically when moved to 18 inches that the efforts to zero the field at 9 inches were ineffective at the 18-inch separation distance. At the 18-inch separation distance, we were somewhat limited by the fact that the signal levels were extremely small and thus the signal-to-noise ratio was much lower. Even more realistic measurements probably should have been made at a greater separation distance if the disturbance at the even lower levels could have been detected in the ambient noise. As stated previously, this was not the case, and thus the measurements at 18 inches were the basis for the compensating windings. The actual incorporation of the compensating dipoles was somewhat limited by

-35-

the spaces available for their incorporation in the unit. This limitation and a slight shift in the location of one added dipole, necessary during final fabrication, proved to result in slight overcompensation when measured at 18 inches from the unit geometric center.

Time limitations restricted additional work in this area, and thus the unit was tested even though it was known we had slightly overcompensated. It should be noted, however, that even more complete compensation could probably be realized with additional testing and compensation design. The location of the compensating dipoles added is indicated in Figure 8. The calculation of the magnitude of and the disturbance due to these dipoles at the test points chosen during the testing at the Magnetic Observatory are calculated in Appendix B. These calculations are given additional consideration in evaluation of the test results of the testing at the Magnetic Observatory.

During testing at the Honeywell Laboratory, it was found that the disturbance due to circulating currents loops was directly dependent on output current and only slightly dependent on input current. The maximum disturbance is generated therefore at full loads, regardless of input voltage. Thus, the compensating dipoles added were made proportional to load current.

3.   Magnetic Disturbance Testing at the Fredericksburg Observatory, 24 - 25 June, 1965

A second series of tests to determine the magnetic disturbance created by the coaxial low input voltage converter regulator (LIVCR) were conducted at the Fredericksburg Magnetic Observatory on 24-25 June 1965. These tests were conducted to verify the improvements afforded by the design changes incorporated to reduce the magnetic disturbance measured during the first series of tests. The first series of tests conducted at the Magnetic Observatory on 3-4 June 1965 indicated two primary problem areas. These problem areas were 1) the output choke coil that was fabricated from mu-metal stock and with a laminar construction and 2) current loops in the regulator section.
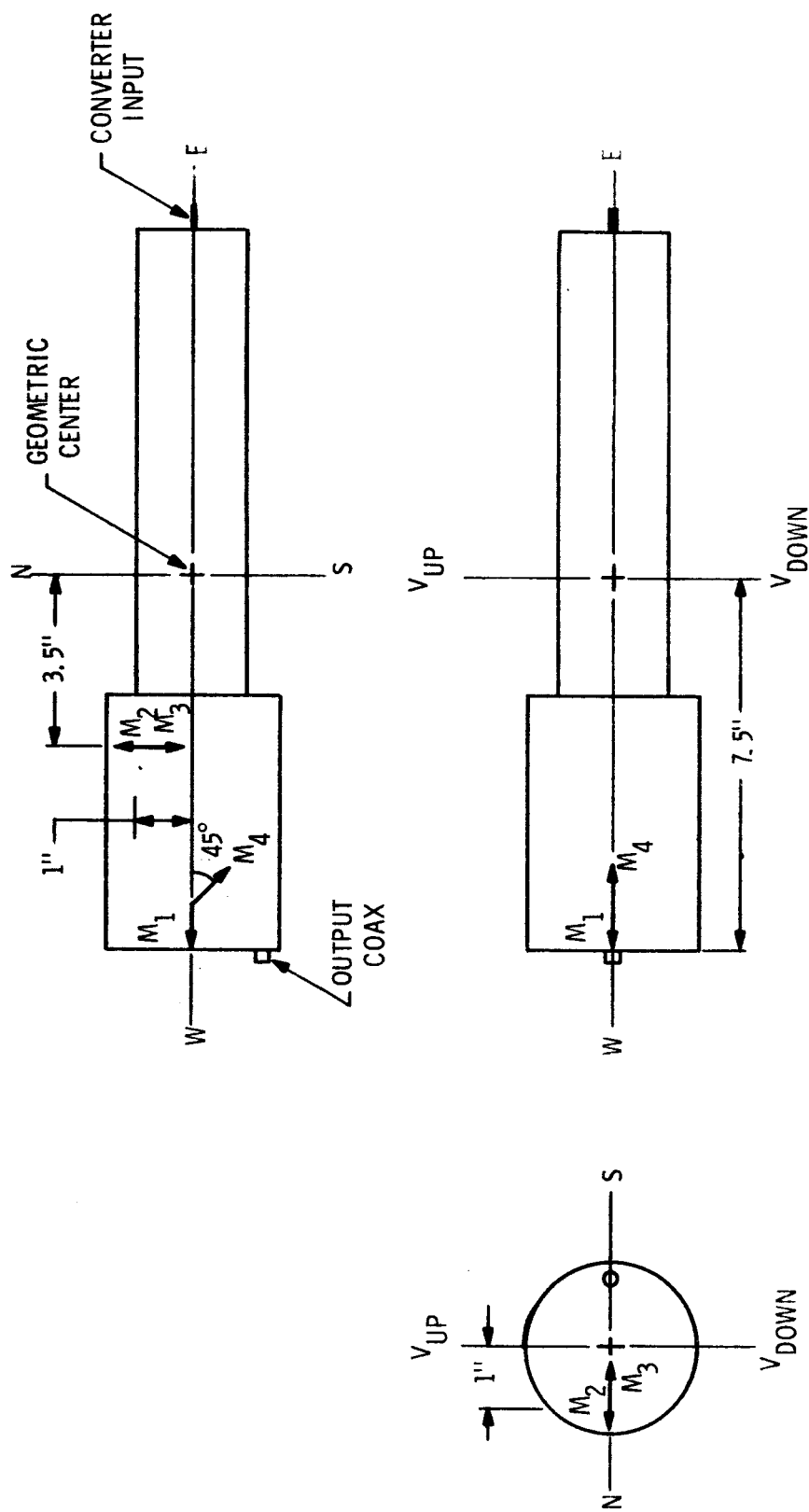
NOTE: M_1 & M_2 ARE CURRENT LOOP COMPENSATING DIPOLES
       M_3 & M_4 ARE DIPOLES REPRESENTING DISTURBANCE DUE TO UNCOMPENSATED UNIT
       LIVCR SHOWN IN 0° POSITION

Figure 8 -- CIRCULATING CURRENT DIPOLE LOCATIONS

Recognizing these problem areas, design changes involving the fabrication of a new choke utilizing a powdered permalloy core and the incorporation of compensating current loops in the regulator section were implemented. Preliminary magnetic disturbance testing was conducted at the Honeywell Ordnance Laboratory to determine if these design changes did result in a reduction of the magnetic disturbance created by the unit under various conditions. Although the tests served as a useful design aid, they were limited by the noise in the area and the inability to completely zero out the earth's magnetic field. Thus, this second series of tests was conducted to obtain more accurate and conclusive information on this improved unit. An abstract of a paper describing the test facility at Fredericksburg is included in Appendix E.

The magnetic disturbance testing procedure consisted of mapping: 1) the initial permanent magnetic field, 2) the permanent magnetic field after 25-gauss exposure, 3) the permanent magnetic field after deperming, 4) the induced magnetic field with 26000 gamma primary field, and 5) the stray magnetic fields due to circulating currents. The first series of tests at the Observatory and the tests conducted at the Honeywell laboratory indicated the axes of maximum disturbance to be those along the longitudinal axes of the coaxial device and along an axes perpendicular to that longitudinal axes at the junction of the converter-regulator section. To facilitate the testing procedure, these axes were most extensively investigated in this second series of tests.

Additional exploratory measurements were made at various points on the surface of an imaginary sphere with a radius of 18 inches from the geometric center of the device to ensure that the axes of this most intensive investigation were truly worst case disturbance axes. A photograph of the LIVCR in the test facility at Fredericksburg is shown in Figures 9A and 9B. The orientation reference for the unit during the testing is indicated in Figure 7. The unit is shown in its zero degree position. The input end of the converter is facing east with the output end facing west. It should be noted that the
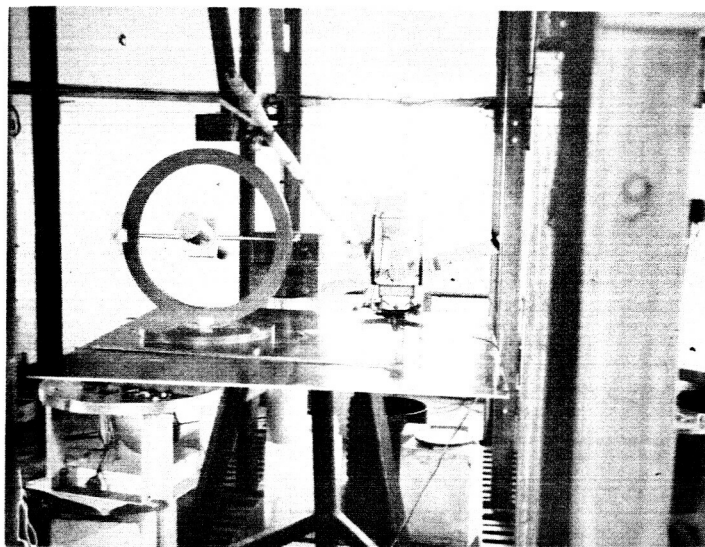
(a)
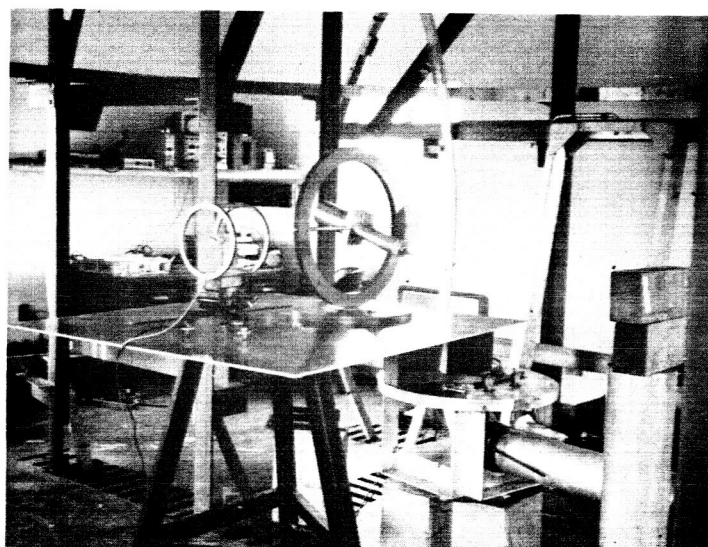
(b)

Figure 9 - FREDERICKSBURG MAGNETIC OBSERVATORY TEST
FACILITY

coaxial output connector is on the south side of the unit's west face in the zero degree position. The directions of rotation about the respective axes were: 1) clockwise looking down for the vertical axis rotation, 2) clockwise when looking south for the north-south axis rotation, and 3) clockwise when facing east for the east-west axis rotation.

It follows therefore, that the 90° position for vertical axis rotation would be with the converter input end pointing south. The 90° position for the north-south axis rotation would find the converter input end facing upward. The 90° position for the east-west axis rotation would find the coaxial output connector in a downward position on the output face of the converter. These points of reference are used to identify the disturbances associated with various converter and sensor orientations indicated in Appendix C.

a.   <u>Initial Permanent Magnetic Field Mapping</u> - The mapping of the initial permanent magnetic field of the coaxial LIVCR was obtained by introducing the unit to the zero field condition and rotating it about each of the three axes perpendicular to the geometric center. The disturbance effected by the unit was recorded on a fluke roll chart, and those points of maximum disturbance were noted on the chart. The disturbance due to the unit under this condition was quite low so special effort had to be made to distinguish the signal from the ambient noise.

It was especially hard to be sure of those signals that were less than 5 tenths of a gamma. The maximum disturbance noted in this condition was approximately 2 gamma. The maximum disturbance points and additional representative points are indicated in Table I, Appendix C. This tabular form for the presentation of the disturbance data rather than an equivalent dipole representation was chosen because of a rather low signal-to-noise ratio. Thus, it seems that extensive calculations to determine dipoles based on this high noise data would be somewhat meaningless and is more realistically evaluated by saying that it is merely somewhat less than a 2 gamma disturbance. Attempts to measure the disturbance at 36 inches resulted in indistinguishable signal levels in the noisy atmosphere.

b.   **Permanent Magnetic Field Mapping After 25 Gauss Exposure** -
Because previous testing on the LIVCR indicated that the initial permanent
magnetic moment was directed along the longitudinal axes, the unit was
exposed to a 25 gauss field directed along this axes. The unit was then
removed from this high gauss field and reintroduced into the zero field
test area. The tests conducted for the initial magnetic field were now
repeated for this post 25-gauss exposure test. The results of this testing
is tabulated in Table II. In referring to this table, it is obvious that the
maximum disturbance realized was indeed due to a dipole directed along
this longitudinal axis previously referenced. The effect of this dipole is
increased due to the fact that it is located in the regulator section, several
inches removed from the geometric center of the device. Because of this,
when the device is rotated about the vertical axis passing through the
geometric center, the actual dipole passes to within approximately 13 inches
of this sensor when in the 270° position. This explains the inequality of
the plus and minus disturbance realized when measuring the disturbance at
18 inches from the geometric center for this rotation.

If the device were rotated about an axes passing through the center of the
dipole, one would find that the plus and minus disturbance would be equal.
Because the zero field condition varied somewhat (in otherwords deviated
from zero), the actual plus and minus disturbance from the ambient was
checked by removing the unit from the test area and then re-introducing it
to the area and noting the disturbance effected by its re-introduction. The
disturbance effected by its re-introduction was then superimposed on that
realized due to the rotation of the device in each axes where the zero degree
position was used for zero reference.

This removal and re-introduction procedure was repeated for ezch of the three sensor orientations. The introduction angle was maintained fixed on the unit for each introduction, as the zero point or zero degree point of each axis is the same. By referring to Table II, one can see that the maximum disturbance realized was +12.0 gamma. The disturbance measured corresponds quite closely with that measured with a removed choke coil in the 3 June tests. This indicates the addition of the permalloy choke coil has not appreciably affected this permanent magnetic field.

Measurements taken 36 inches from the geometric center and along this worst case ases indicated that the disturbance was something less than ± 1 gamma. This rather significant reduction in the field strength is not a violation of the inverse cube law which at first may seem to be the case. Even though the separation distance between the sensor and the geometric center has only been doubled, the separation distance between a sensor and the effective dipole of the unit has been increased by a factor of approximately 2.4. (Refer to dipole location calculated in Appendix A.) The measurements as tabulated in Table II were taken on 24 June 1965. However, the measurements indicating the greatest disturbance were repeated on 25 June to increase the confidence in and check the validity of them. Because measurements on the two days compared quite favorably, they appear to be valid.

c.   Permanent Magnetic Field Mapping After Deperming - When the mapping of the magnetic field due to the unit after 25-gauss exposure was completed, the unit was depermed by exposing it to a field generated by a steadily decreasing alternating current. This field was decreased from an intensity of approximately 50 gauss down to near zero field. The magnetic testing procedure was then once again repeated. The disturbance realized was even lower than that due to the initial permanent magnetism. The meager data obtained where the signal was significant compared to the noise is presented in Table III. For the majority of the testing, the signal was lower than the noise and thus could not accurately be determined. It is apparent, however, that the disturbance generated is sonewhat less than ± 1 gamma.

d. <u>Induced Magnetic Field Mapping with 26,000 Gamma Primary Field</u> - Following the depermed magnetic field tests, the induced magnetic field with an 26000 gamma primary field in the vertical direction was mapped. This mapping consisted of the induced magnetic field only in the horizontal plane, for it was impossible to detect gammas of disturbance from a 26000 gamma ambient. The ambient conditions were essentially 26000 gamma in the vertical plane and zero gamma in the horizontal plane. The testing was conducted to determine if the introduction of the unit would bend the vertical flux lines such that a disturbance could be detected in the horizontal plane.

The noise levels associated with this test proved to be especially high because even slight variations in the vertical field also affected the so-called zero field conditioned in the horizontal plane. This condition is due to the fact that the vertical coils were not exactly orthogonal with the horizontal coils, and thus some small field with variations was generated in the horizontal due to the vertical field and its variation. Careful and repeated testing in this atmosphere, however, did yield realistic test data. The measurements associated with each LIVCR rotation and sensor orientation were repeated several times. Efforts were made to separate the signal from the noise by correlating measurements taken for corresponding test conditions. Special cognizance was taken of the maximum disturbance associated with each test condition and their repeatability to distinguish the maximum disturbance from the random magnetic noise.

It was found that the disturbance in the horizontal plane was somewhat less than ± 2 gamma. Once again the exact magnitude of the disturbance was very difficult to determine. No attempt was made to measure the disturbance at a geometric center of the LIVCR to sensor separation of 36 inches.

e. Stray Magnetic Fields Due to Circulating Currents - The measurement of the magnetic field associated with circulating currents were made in a zero field region. These tests provided a map of the maximum difference in the magnetic field associated with power on - power off conditions of the package. The input and output power was cabled to and from the device with coaxial lines to reduce the disturbance due to them. The magnetic field due to the high input currents was also accounted for by shorting the input line directly at the input to the converter and forcing currents through the input lines equal to the input current of the running device. The input line disturbance under the shorted condition was then subtracted from the disturbance due to the input line and the LIVCR when running. This allowed the isolation of the disturbance due to the LIVCR. The slight disturbance generated by load current flowing through the coaxial output lead which had some eccentricity was not zeroed out, but this appeared to be rather small. Due to the long, inflexible input lead, the rotation realized for this series of tests was only around the east-west axis of the converter. To more fully investigate the magnetic field generated by the device, however, the sensor was positioned at several points around the device.

A reasonably complete sampling of test points around the LIVCR indicated that the maximum disturbance could be realistically represented by the measurements indicated in Table V. Referring to Table V, it can be seen that these measurements were taken with the sensor located in two respective positions while the converter was rotated around its east-west, or longitudinal axis. The disturbance measured for the three sensor orientations and its two respective locations did not exceed ± 11 gamma.

Most of the measurements were in the less than 5 gamma range. It is significant to note that the over compensation noted in the testing at the Honeywell Laboratory was again apparent in the data presented here. This is probably best shown in the measurement taken with the sensor located 18 inches west, with the sensor oriented east-west, and the LIVCR oriented at the 180° position around its east-west rotation axis. For this orientation, the disturbance measured is +9 gamma. The disturbance measured when the compensating coils were disconnected was -23 gamma. Thus, the overcompensation for this test point is 9 gamma. For the same unit and sensor orientations but a separation distance of 36 inches, the disturbance measured was less than ± 0.5 gamma with the compensation in, but was in the 2 gamma range with no compensation. Various other points may be compared by referring to the tabulated data in Table V.

Probably a more descriptive presentation of the disturbance measured is presented in Figure 10. The information presented here is essentially the same as that of Table V, the exceptions being that for this presentation it is assumed that the sensor is moved with respect to the fixed converter. This merely involves choosing a new reference for the field vectors and involves no additional testing. For example, in transforming the measurements presented in Table V to the presentation of Figure 10; the vertical-up direction with the sensor located 18 inches south and the unit rotated about its east-west axis becomes 1) the vertical-up direction for point B, 2) a south direction for point E, 3) the vertical down position for point D, and 4) the north direction for point C, respectively. Also, it should be noted that the measurements indicated for 18-inch west sensor located in Table V has been resolved into a single representation in Figure 10. The measurements taken while the converter was rotated provided a check on individual measurements. One would normally expect the magnitude of the disturbance in the plane perpendicular to the longitudinal axis to remain constant while the direction only changed with the rotation for this sensor location (18" west).

-45-
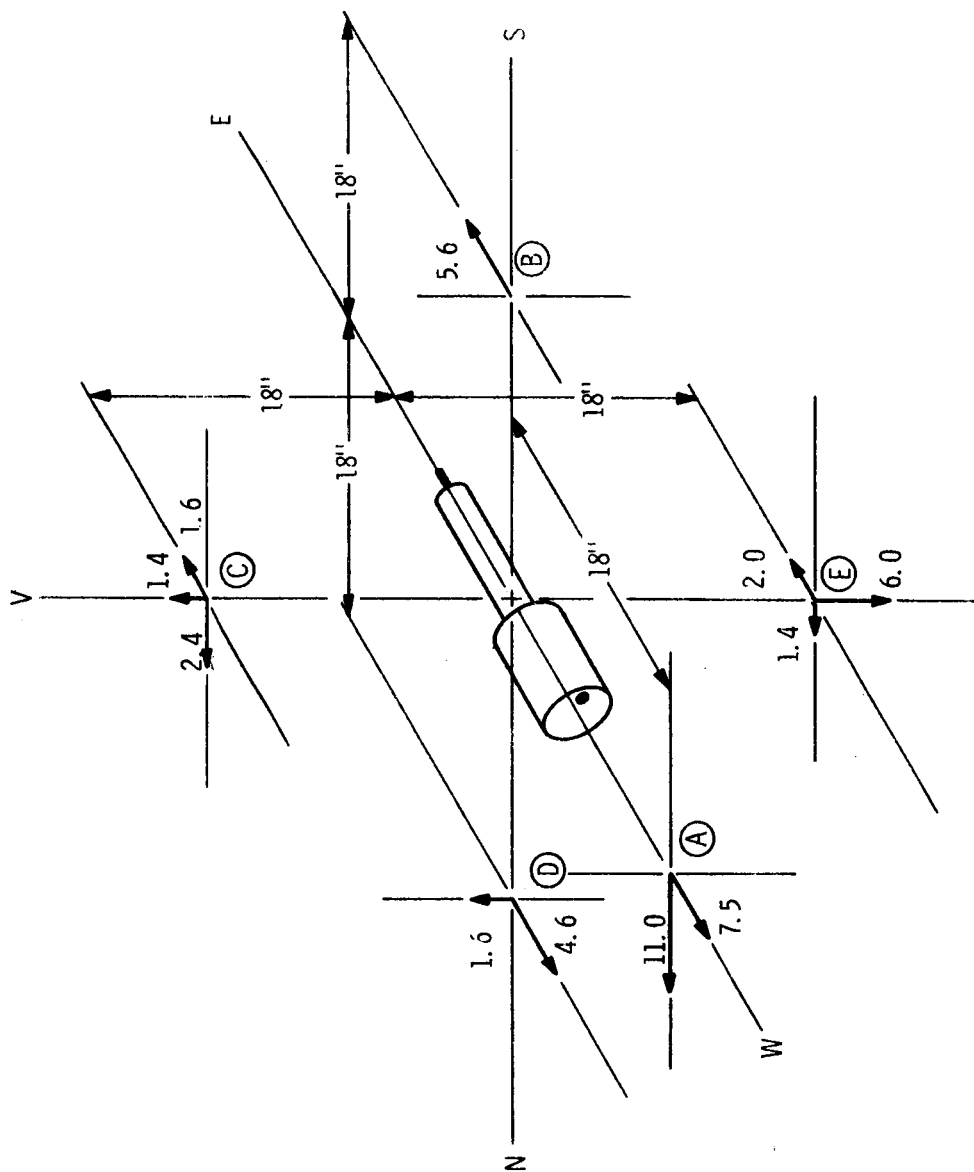
NOTE: DISTURBANCE IN GAMMAS
TEST POINTS INDICATED BY ENCIRCLED LETTERS
TESTS CONDUCTED JUNE 24, 1965
LIVCR OPERATING AT FULL LOAD

Figure 10 – LIVCR EXG 2424N1X1 POWER ON/POWER OFF MAGNETIC
FIELD DIFFERENCE

-46-

For example, in Table V, the disturbance in the vertical axis for the 0° and 180° unit orientation should be of the same magnitude as the disturbance in the north-south axis for the 90° and 270° orientation. Likewise, one would expect the disturbance in the east-west axis to remain constant with unit rotation. This, however, was not the case. This discrepancy may have been due to several factors: 1) an inexact positioning of the sensor on the longitudinal axis of the device, 2) slight changes in the effects of the input and output leads not completely accounted for, and 3) changes in the ambient magnetic field.

Because of this discrepancy, the four respective measurements taken for each vector component, as presented in Table V, were averaged for the presentation of Figure 10. The evaluation of these measurements is somewhat complicated because the measurements at the 18-inch separation cannot be represented by a simple generating dipole; this is especially true for test point A.

The approach taken to evaluate this data was to first calculate the disturbance due to the compensating dipoles added to the LIVCR (see Appendix B). The result of subtracting the calculated disturbance from the compensated device disturbance measured is presented in Figure 11. In addition to this net magnetic field difference with no compensation in the converter as calculated, the magnetic disturbance measured with the compensating windings disconnected is included in boxed in numbers. While it is felt a vigorous determination of the generating dipoles causing a disturbance as indicated is not merited, an approximation to these dipoles is considered. Slight discrepancies may be noted in the difference first arrived at by subtracting the calculated disturbance for the compensating dipoles from the measured disturbance of the compensated device; and, secondly, that disturbance measured from the device with no compensation. It therefore appears that either there are slight errors in the measurements, or that small magnetic materials in the device are slightly distorting the effects of the compensating dipoles. By approximation in a limited trial and error procedure, the approximations to the actual LIVCR dipoles with no compensation were determined as shown in Appendix D.
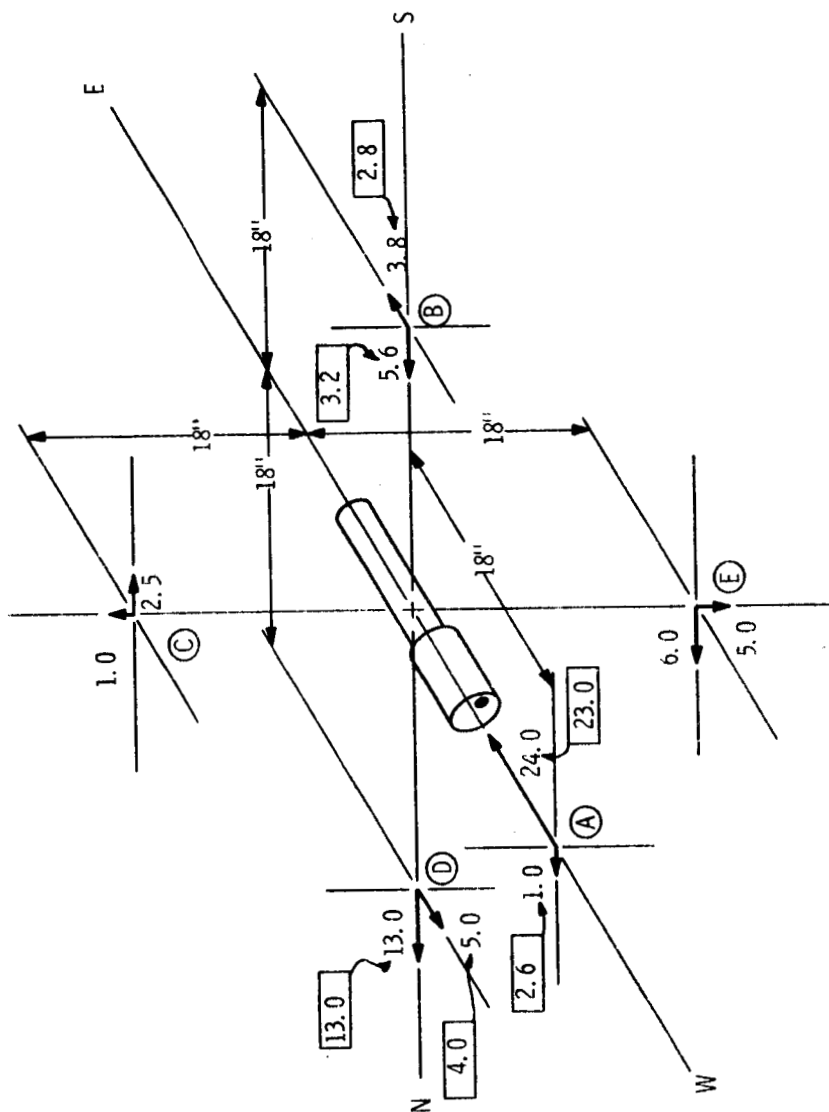
NOTE: DISTURBANCE IN GAMMAS
(1) NUMBERS ENCLOSED IN BOXES INDICATE MEASURED DISTURBANCE.
(2) NUMBERS NOT ENCLOSED WERE DETERMINED BY SUBTRACTING THE CALCULATED
DISTURBANCE OF THE COMPENSATING DIPOLES FROM THE MEASURED DISTURBANCE
OF THE COMPENSATED LIVCR.

TESTS POINTS INDICATED BY ENCIRCLED LETTERS
TESTS CONDUCTED JUNE 24, 1965.
LIVCR OPERATING AT FULL LOAD.

Figure 11 - POWER ON/POWER OFF MAGNETIC FIELD DIFFERENCE
WITH NO COMPENSATION

-48-

The following discussion determines unaccounted magnetic disturbance by subtracting the disturbance contributed by M_1, M_2, M_3, and M_4 from the disturbance measured from the compensated LIVCR. Refer to Figures 10 and 11. Differences in the measured and calculated effects of M_1 and M_2 are indicated below by enclosing measured effects in brackets. Disturbances are indicated in gamma.

Test Point (A)

Component	Vertical	NS	EW
LIVCR Disturbance	0	11 N	7.5 W
Minus $M_1 + M_2$ Disturbance	0	-9.9 N	-31.5 W
Minus $M_3 + M_4$ Disturbance	0	-1.1 N	-24.0 E
Unaccounted for Disturbance	0	0	0

Test Point (B)

Component	Vertical	NS	[NS]	EW	[EW]
LIVCR Disturbance	0	0	[0	5.6 E	5.6 E]
Minus $M_1 + M_2$ Disturbance	0	-5.6S	-3.2S*	-1.8 E	-2.3E*]
Minus $M_3 + M_4$ Disturbance	0	-3.6N	-3.6N	- .5 E	-0.5 E]
Unaccounted for Disturbance	0	2.0N	0.4S]	3.3 E	2.3E]

*Note: measured data

Test Point (C)

Component	Vertical	NS	EW
LIVCR Disturbance	1. 4 Up	2. 4N	1. 6 E
Minus $M_1 + M_2$ Disturbance	-0. 6 Up	-5. 0N	-1. 9 E
Minus $M_3 + M_4$ Disturbance	-0. 4 Down	-3. 3S	-1. 2W
Unaccounted for Disturbance	1. 2 Up	0. 7N	0. 9 E

Test Point (D)

Component	Vertical		NS		EW	
LIVCR Disturbance	1. 6 Up	1. 6 Up	0	0	4. 6W	4. 6W
Minus $M_1 + M_2$ Disturbance	0	-1. 6 Up*	-13. 4S	-13 S*	-0. 7 E	-0. 6W*
Minus $M_3 + M_4$ Disturbance	0	0	-11. 3N	-11. 3N	0. 4W	-0. 4W
Unaccounted for Disturbance	1. 6 Up	0	2. 1N	1. 7N	4. 9W	3. 6W

Test Point (E)

Component	Vertical	NS	EW
LIVCR Disturbance	6 Down	1. 4N	1. 2E
Minus $M_1 + M_2$ Disturbance	-0. 6 Down	-5. 0S	-1. 9 E
Minus $M_3 + M_4$ Disturbance	-0. 4 Up	-6. 7N	-1. 2W
Unaccounted for Disturbance	5. 8 Down	0. 3S	0. 5 E

*Note: measured data.

The preceding determination indicates that the disturbance has been accounted for reasonably well. The exceptions to this are the disturbances in the vertical direction at test point (E) and in the EW direction at test point (D), which probably could be accounted for with additional work. It is significant that this unaccounted disturbance at (D) is different when considering the measured or calculated effects of M_1 or M_2.

Because the original measurement at point (E) seems somewhat inconsistent, the validity of it is questioned. The proportionally large vertical disturbance component was not recognized while the actual testing was conducted, and a confirming re-check at this point was not conducted. The important point, however, seems to be that the net disturbance can be approximated by generating dipoles reasonably well, and these dipoles cannot be resolved into a single dipole when considering the "near field" disturbance at 18 inches from the LIVCR geometric center. Because of this, the decrease in disturbance with increasing separation distance (from 18 inches) should be even greater than the inverse cube relationship characteristic of a single dipole.

f.   Component Magnetic Disturbance Testing - In conjunction with the magnetic disturbance testing of the LIVCR at Fredericksburg 24-25 June 1965, the permanent magnetic field after 25-gauss exposure of a few components was investigated. The components considered included 1) a "non-magnetic" 2N2833 germanium transistor, 2) a standard 2N2833, 3) a 2N297 transistor, 4) a 2N718 transistor, 5) a "Deltamax" toroidal core, and 6) a "Supermalloy" toroidal core. For these tests, the components were first exposed to a 25-gauss field and were then introducted to the zero field test area and rotated at a sensor to component sepatation of 13 inches. This separation distance was chosen because the center of the LIVCR regulator section passes within 13 inches of the sensor during testing of the LIVCR disturbance. The transistors tested are located in this area, and, therefore, this component testing should provide a basis for evaluating the disturbance of the LIVCR. The maximum disturbance of the components are tabulated below.

-51-

Component	Magnetic Disturbance (gamma)	Sensor to Component Separation
"Non-Magnetic" 2N2833 - (TO-3)	± 7	13 inches
Standard 2N2833 (TO-3)	± 7	↑
2N697 with 1.5" leads (TO-5)	± 15	
2N718 with 1.5" leads (TO-18)	± 3	
2N718 with 0.1" leads (TO-18)	± 1	
Deltamax Core (35E-4602)	±1.5	↓
Supermalloy Core (35E-8602)	0	13 inches

Figure 12 - COMPONENT MAGNETIC DISTURBANCE

The "non-magnetic" 2N2833 is obviously magnetic, probably due to the nickel used to plate the otherwise non-magnetic construction. The non-magnetic 2N2833 contains magnetic leads and may also contain magnetic material inside the copper case. It is apparent that the leads on the 2N697 and 2N718 transistors contribute appreciable disturbance. Several transistors are used in the regulator section which have TO-5 or TO-18 cans. Also, one standard 2N2833 transistor is used in this section. (True non-magnetic transistors were not available.)

Referring to Table II and the disturbance of the LIVCR measured after 25-gauss exposure, it can be seen that the disturbance of the LIVCR is 12 gamma when the regulator is rotated near the sensor. The component disturbance above indicates that the transistors are a prime source of this disturbance. It should be noted that the transistor leads were cut short in the LIVCR to minimize their disturbance. The testing of the "Deltamax" and "Supermalloy" core was conducted only for academic reasons and for verification of theoretical conclusions. No Deltamax material was used in LIVCR EXG 2424 N1X1.

It can be noted that the transistors which had low magnetic mass produced many times the magnetic disturbance of the toroidal cores which had a relatively large mass but were fabricated from high permeability, low residual materials.

H. PERFORMANCE

Performance tests showed that the coaxial design and circuit modifications resulted in an improvement in over-all performance. The coaxial design substantially reduced the inductance of the high current buss work and the input lead, and this reduction minimizes the generation of voltage spikes at the input when the power oscillator switches. Voltage spikes at the power oscillator input increase the voltage current product during the switching interval and hence increase the power oscillator switching losses. Minimization of the input inductance with the coaxial design reduces these voltage spikes and the switching losses. In addition, circuit improvements have decreased the power oscillator switching time. The reduction in the magnitude of the voltage spikes and the reduction in the switching duration have resulted in a substantial reduction in switching losses. This reduction has provided higher efficiency and has allowed the use of higher operating frequencies that facilitate weight reduction. Thus, the coaxial design has provided additional advantages besides the minimization of magnetic disturbance.

The low voltage converter-regulator performance was checked over the input voltage and load range while operating at ambient temperatures of 25° C, -10° C, and 70° C. The performance of the device operating in these ambient temperatures is shown on Figures 13, 14, and 15, respectively, and in the data shown in Appendix F.
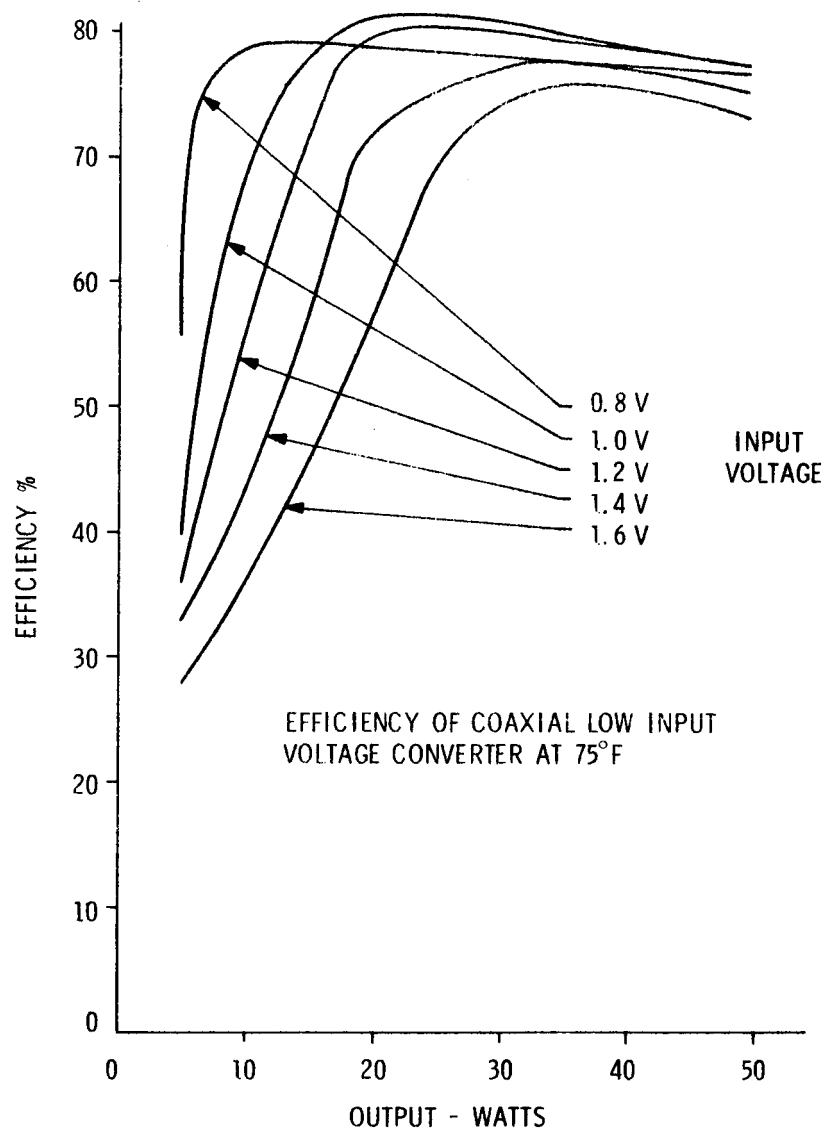
Figure 13 - EFFICIENCY CHARACTERISTICS OF COAXIAL LIVCR
EXG 2424N1X1 (25°C)

EFFICIENCY OF COAXIAL LOW INPUT
VOLTAGE CONVERTER AT 14°F
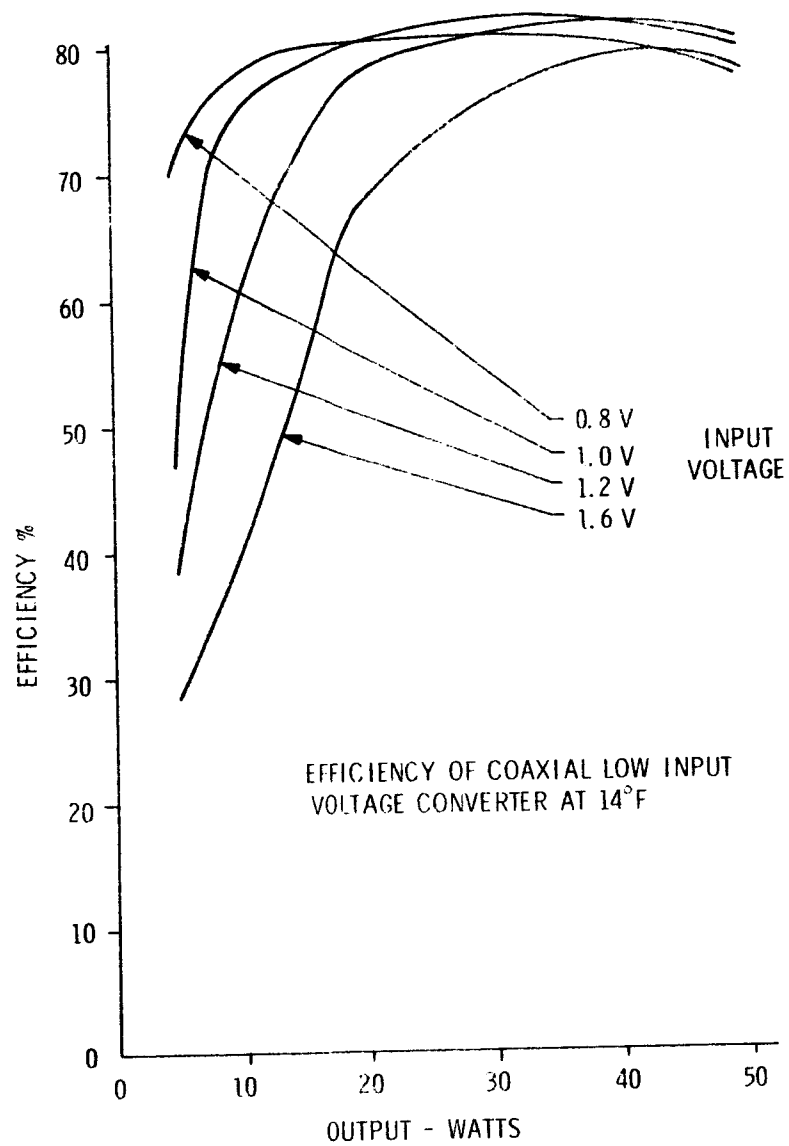
Figure 14 - EFFICIENCY CHARACTERISTICS OF COAXIAL LIVCR EXG
2424N1X1 (-10°C)
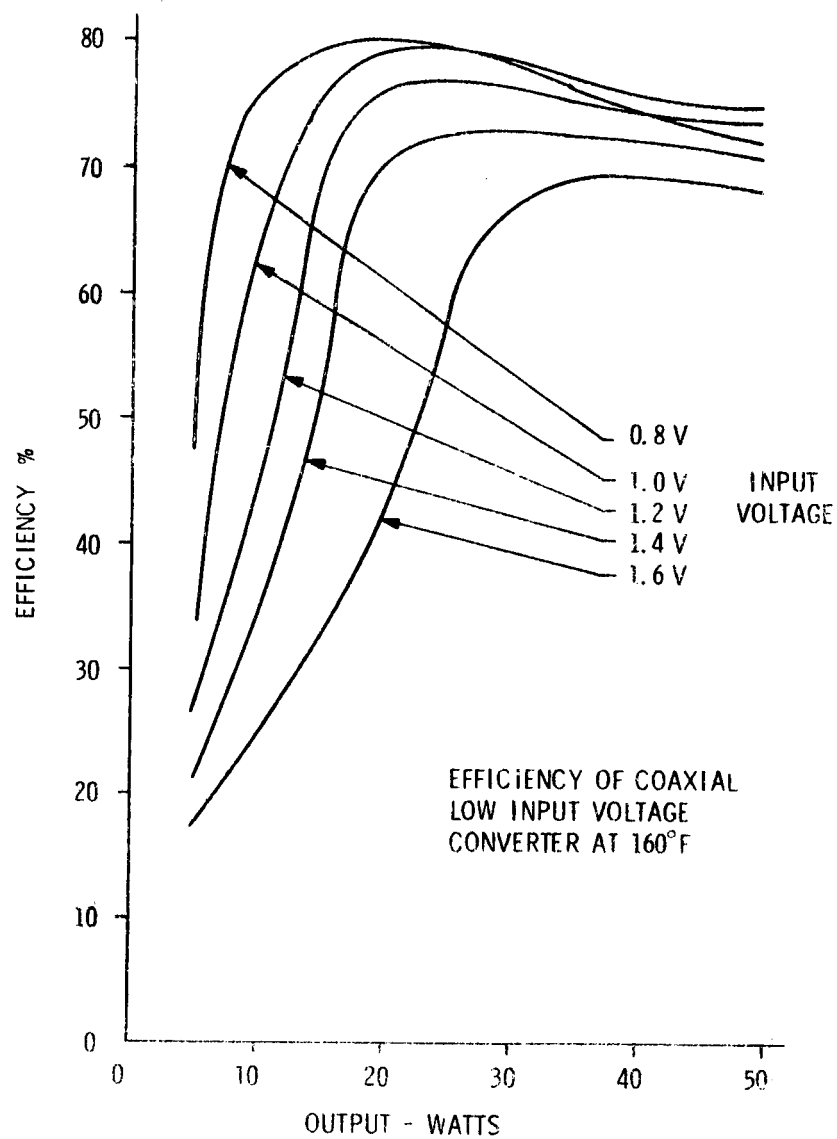
Figure 15 - EFFICIENCY CHARACTERISTICS OF COAXIAL LIVCR
EXG 2424N1X1 (+70° C)

Examination of Figure 13 shows that at lower input voltages the efficiency was higher at lighter load, and conversely, at the higher input voltage, the light load efficiency was lower. This reduced efficiency is caused by a higher operating frequency, at higher input voltages, producing switching losses and increased core loss. The operating frequency varies between 900 cps at 0. 8 volts full load to 3000 cps at 1. 6 volts light load. Note that at 0. 8-volt input the efficiency remains above 76% over an 8- to 50-watt load range.

A peak efficiency of 81% is obtained with a 1. 0-volt input at a 25-watt load. At 50 watts load, all efficiencies are above 75%, except for the 1. 6-volt input curve which is 73%. When the device is connected for a 1. 2 to 1. 8 input voltage range by changing transformer taps inside the regulator section, an efficiency of 75% can be achieved with a 1. 6-volt input and a 50-watt load. Because these connections are inconvenient to make, the unit is normally operated on the 0. 8- to 1. 6-volt range top only.

Operation at -10° C. provides higher overall efficiencies as shown on Figure 14. The efficiencies at 50 watts load range between 77. 5 and 81% for inputs between 0. 8 and 1. 6 volts. The higher efficiencies at lower temperatures are probably caused by lower copper resistance and changes in the transistor characteristics. On the average, the efficiencies are approximately 3% higher at -10° C than they are at 25° C.

The LIVCR performance at 70° C, illustrated on Figure 15, shows that the efficiency declines due to the higher ambient temperature. These efficiencies are 3 to 5% lower than the values obtained at 25° C.

The lower efficiency is probably due to increased copper resistance and changes in transistor parameters at the higher temperature.

On the above performance curves, it can be noted that the efficiency remains relatively high throughout the wide input voltage and load range. The maintenance of the high efficiencies throughout these ranges is due to the use of the current feedback power oscillator, which provides the optimum drive to the power oscillator for all input voltage, load, and ambient temperature conditions. The pulse width modulation voltage regulator utilizes current drive for the pulse modulating transistor, maintains high efficiency, and provides the desired regulated 28-volt dc output throughout the wide operating ranges. Besides minimizing the external magnetic field disturbance, the coaxial construction and coaxial input lead minimizes the input and primary circuit inductance. This feature reduces input voltage spikes, reduces transistor switching losses, increases efficiency, and allows higher frequency operation thereby facilitating weight reduction.

The curve on Figure 16 shows the overload characteristics of the low voltage converter-regulator. Note that the device voltage declines nearly linearly with load and that a relatively high efficiency is maintained even in the heavy overload condition. Since the efficiency remains high under overload and the input power is reduced to a very low value when the output is shorted, the device is capable of continuous operation when the output is overloaded or shorted. The overload current limiting circuit has fast response and protects for slowly increasing overloads as well as for sudden dead shorts. It also recovers immediately when the overload is removed and supplies rated power to the normal load.

I. CONCLUSION

The work during this program has produced significant improvements in the low input voltage converter-regulator technology. This effort has resulted in design techniques which minimize the external magnetic field disturbance and provide other benefits as well. Basically, significant improvements have been made in the following areas:
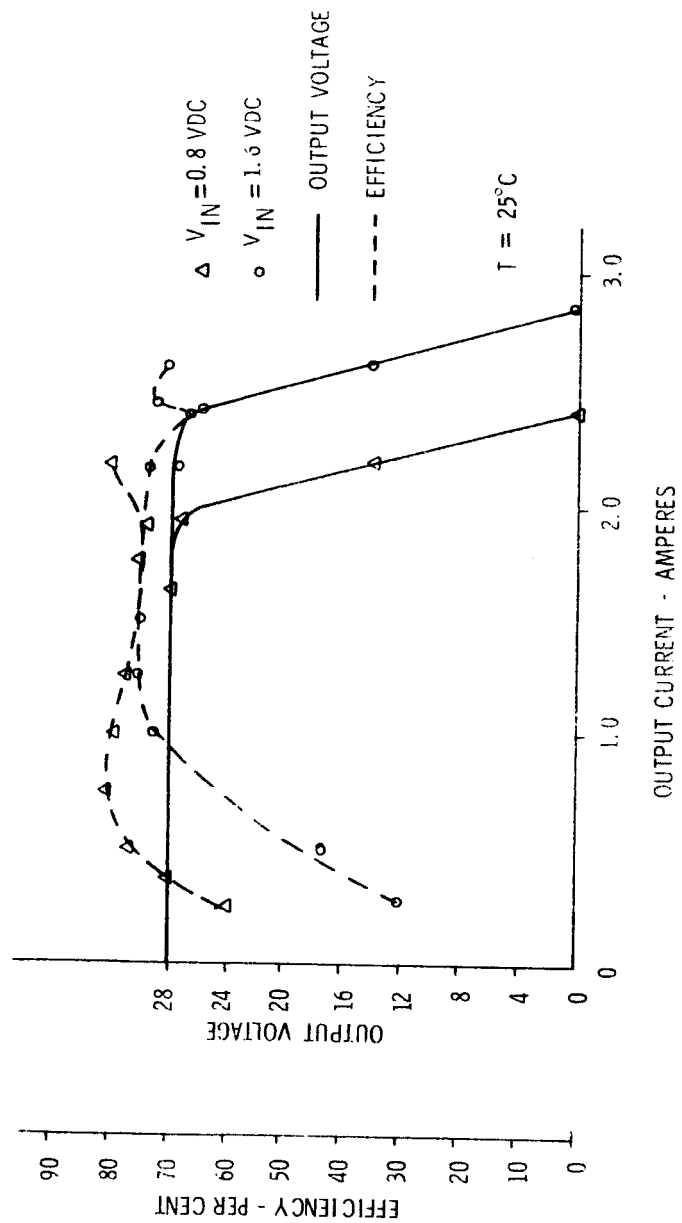
Figure 16 - OVERLOAD CHARACTERISTICS OF EXG 2424N1X1

1. Improvements in the current feedback power oscillator that allow the conversion of low voltage, high current power to ac or dc at higher efficiency and higher frequencies, which facilitate weight reduction.

2. Improvements in the power oscillator transformer construction that diminish the effects of effective dc magnetizing current components on the power oscillator performance.

3. Improvements in the voltage regulator that provide a better current drive for the chopping transistor, and snap acting circuitry that provides higher back bias power to improve regulator switching and temperature stability.

4. A coaxial low voltage converter design that minimizes the external magnetic disturbance and also minimizes the inductance of the input lead and primary circuit. Thus, besides minimizing magnetic disturbance, the reduction of input inductance is also beneficial because it reduces input voltage spikes, thereby reducing transistor switching losses and diminishing the voltage stress applied to the oscillator transistors.

The improvements in the current feedback power oscillator circuitry have provided a means of back biasing the switching "off" transistor to a higher voltage, which tends to sweep the stored carriers out of the base region more rapidly and accomplishes more rapid transistor switching.

The low saturation voltage transistors used such as the MHT 2305 typically have long storage times, and in previous circuitry, switched slowly when back biased to only 0. 45 volts.

The new circuitry momentarily provides a back bias of 2 to 3 volts for 10 to 20 microseconds to speed oscillator switching. This feature has been accomplished without the use of dissipative components that would diminish efficiency in low voltage, high current applications. The faster transistor switching afforded by this circuit has reduced switching losses and allowed more efficient operation at higher frequencies where weight reduction can be achieved.

The operating frequency of the low voltage converter delivered under this contract ranges between 900 and 3000 cps over the load and 0.8 to 1.6 input voltage range. Performance data has verified that the efficiency has been improved, in general, this circuitry has increased the efficiency by approximately 5% when operating at 1000 cps.

Circuit investigations have shown that a slight unbalance in the voltage time integral of succeeding power oscillator half cycles can result in an effective dc component that operates the core toward one side of the hysteresis loop and causes the core to saturate toward the end of one-half cycle. This mode will result in a high input current spike, which increases the energy stored in the input inductance and increases the transistor dissipation during switching due to a higher voltage-current product during switching. The high collector current surge also slows switching to further increase dissipation. Investigations during this program have shown that this effect can be greatly diminished by incorporating an air gap in a portion of the magnetic circuit cross sectional area. Performance tests have verified that this technique greatly diminishes this effect and improves device efficiency. These techniques were incorporated into the model delivered at the end of this program.

The voltage regulator bias circuit improvements have improved the over-all efficiency by providing a better drive to the chopping transistor under all conditions. This improvement has eliminated the need to design the device for the worst-case conditions, which resulted in excessive drive losses under most other operating conditions. The incorporation of snap acting back bias circuitry has increased the chopping transistor switching speed; thereby reducing switching losses, facilitating operation at higher frequencies and improving temperature stability.

The coaxial low input voltage converter design minimizes external magnetic disturbance because the external magnetic disturbance from the high input current through one lead is canceled by an equal and opposite field from current flowing through the return coaxial conductor. If the concentricity of the two coaxial conductors is held to a few thousandths of an inch, the cancellation will be complete and the magnetic disturbance will be minimized.

Magnetic disturbance tests discussed below verify that this design approach results in minimization of external magnetic field disturbance. In this design, it has been necessary to minimize the magnetic fields due to current loops in all leads carrying more than a few milliamperes by very close spacing of principal and return leads, using techniques such as twisted pairs or coaxial conductors.

This design has been directed towards the use of non-magnetic components where practical and towards the use of very high permeability magnetic materials where necessary for the transformers and reactors. Performance tests indicate that the supermalloy and 4-79 molybdenum permalloy toroidal cores used produce very low external magnetic disturbance. Considerable difficulty was encountered in fabricating a mu-metal choke coil with a totally enclosed air gap. Although this design should have given minimum external magnetic disturbance, it did not because cold working of the material during fabrication deteriorated the magnetic characteristics and caused magnetic disturbance. Tests verified that the choke coil, which was fabricated in this manner, was unsatisfactory, it was replaced by a toroidal choke coil wound on a 4-79 powdered permalloy core. This unit was found to be much more satisfactory.

Although effort was made to obtain transistors with non-magnetic cases, they were not readily available in some types without a great increase in cost. Measurements have shown that the magnetic disturbance in the low voltage converter-regulator are primarily concentrated in the regulator. Additional measurements have shown that the magnetic cases and leads in the standard 2N2833 and 2N718 transistors are the main cause of magnetic disturbance in the regulator.

It can be concluded that the use of transistors having magnetic cases and leads is the major cause of magnetic disturbance in the converter-regulator model. If these semiconductors could be replaced by non-magnetic equivalents, the magnetic disturbance noted in the regulator section of the LIVCR could be greatly reduced.

Besides minimizing the external magnetic disturbance, the concentric coaxial construction also minimizes the inductance of the input lead and primary circuit. This minimizes the generation of voltage spikes at the input and across the power oscillator transistors by the collapse of energy stored in the input inductance during switching. The reduction of these voltage spikes reduces switching losses because the current voltage product across the transistor during switching is greatly reduced. This feature also reduces the magnitude of voltage stress across the transistor during switching. This is an important feature because the voltage rating of the low saturation transistors used is normally quite low, and, hence, excessive voltage spikes at the input cannot be tolerated.

The maximum external magnetic field disturbance of the coaxial LIVCR, EXG 2424 N1X1, compares favorably with the design goals outlined in PC61309 for the Perm Initial, Post Deperm, and Induced test conditions. These design goal limits are exceeded for the post 25-gauss exposure and Stray power "on" vs. power "off" conditions. The limits are exceeded primarily for the measurements at 18 inches from the geometric center

-63-

of the LIVCR where the limit is 2 gamma. These design goals as outlined in PC61309 are quite stringent, especially for a package with the geometric shape of this coaxial LIVCR; therefore, it was requested that the magnetic measurements on this device should be compared with the more recent Magnetic Test Criteria for IMP Subassemblies and Spacecraft[1].

The test criteria as specified for IMP is reproduced in Tables I and II. Comparing the disturbance measurements presented in Appendix C Tables I through V with the IMP Subassembly criteria, it is apparent that the measurements compare very favorably. The maximum measured disturbance at 18 inches is (1) only 35% of the criteria for the initial perm condition, (2) 40% of the criteria for the post 25-gauss exposure, (3) 50% of the criteria for the post 50-gauss deperm, and (4) exceeds the criteria in the stray "power-on" vs. "power-off" condition. It should be noted, however, that the disturbance is less than the criteria when measured at 36 inches under all test conditions. This is of special significance as it reveals the effects of the geometry of the LIVCR package in relation to the test specification that requires that measurements be taken at distances measured solely from the geometric center of the device. This results in a measurement of the disturbance due to several distinguishable generating dipoles when considered at 18 inches; however, when considered at 36 inches the disturbance can most likely be assumed to be generated by a single dipole that is the vectorial sum of the individual dipoles. At 18 inches, a "near" field (consisting of dipoles of finite dimensions in relation to the distance to the point of measurement) is being measured; at 36 inches the field characteristic tends to approach that of a "far" field (point source).

---

[1]Norman F. Ness, "Magnetic Field Restraints for IMP's F and G", July 9, 1964, p. 9.

Table I

Magnetic Test Criteria for IMP Subassemblies

Condition	Applied Field (gauss)	Maximum Magnetic Field Disturbance (Gamma)	
		18 inches	36 inches
1. Initial Perm.	0	8	1
2. Post 25 gauss exposure	0	32	4
3. Post 50 gauss deperm		2	0.25
4. Stray-"Power on" Vs. "Power off"	0	4	0.50

Table II

Magnetic Test Criteria for IMP Spacecraft

Condition	Applied Field (gauss)	Maximum Field Disturbance (Gamma) 36 inches
1. Initial perm	0	1.0
2. Post 25 gauss exposure	0	10.0
3. Post 50 gauss de perm	0	1.0
4. Stray-"Power on" Vs. "Power off"	0	1.0

If a "far" field were characteristic at both 18 and 36 inches, the disturbance should decrease by a factor of 8 when the separation distance is doubled (18 to 36 inches). The measured results indicate a greater reduction in the field, and thus a "near" to "far" field condition is implied. (This great reduction is also due to the actual location of the dipoles and will be discussed later.)

It is recognized that zero points may exist in a "near" field condition such that increasing the distance from the test point to the device on a collinear line results in increased disturbance. This zero point may be located near a relatively weak dipole that is opposite in direction to a strong dipole located a greater distance away. As the test point is moved away from the weak dipole on a line collinear with the two dipole moments, the flux generated by the larger dipole will become more significant. This is because the inverse cube law applied to each dipole reduces the field intensity due to the weak dipole faster than that due to the strong dipole. Therefore, the field intensity begins to increase before it again decreases.

The situation characteristic of the LIVCR "near" field to "far" field transformation, however, results, as indicated in the measurements, in a field intensity reduction greater than that expected if the far field characteristic were present for both test point distances. This has also been verified by testing at the Honeywell Laboratory.

This can be caused by two dipoles located some finite distance apart having equal but opposite moments. As the test point separation becomes large with respect to the distance between dipoles, the field cancellation becomes more complete and the net disturbance approaches zero. In this case, the field intensity reduction with test point separation is greater than predicted by the inverse cube law.

The major dipoles are located in the regulator section, which is approximately 5 inches long and 3 inches in diameter. Assuming that a dipole is located at each end of the regulator section, it is easy to see why the magnetic field more closely approximates a "far" field characteristic at a test point separation of 36 inches.

In addition to the change in field characteristic, the great reduction in intensity with increasing separation distance from the geometric center is due to major dipoles being located off the geometric center. These major dipoles are located in the regulator section. Thus, doubling the test point separation from 18 inches to 36 inches may result in increasing the distance from the largest dipole by a factor of 2.6. The reduction in field intensity is therefore by a factor equal to the cube of 2.6 when measured off the regulator end along the longitudinal axis.

The measurements at 36 inches seem most meaningful because of the discussed conditions. Exact measurements were not obtained at 36 inches because of the low signal-to-noise ratio; however, the measurements obtained did indicate disturbances less than 0.5 gamma at 36 inches for all test conditions. Note that the criteria for the spacecraft is stated only for 36 inches.

The post 25 gauss exposure LIVCR field appears to be primarily due to a perm retained by various transistors in the regulator section.

The circulating current field is primarily dependent on load currents flowing in the regulator section and relatively independent of input voltage. The disturbance of the converter section therefore appears to be very low. To compensate for the regulator dipoles, dipoles proportional to load current were added. The measurements taken indicate a slight over-compensation for the measurements at 18 inches but was not detected at 36 inches. Additional work in this area consisting of successive tests and modifications, however, would result in additional improvements.

In comparing the measurements for the uncompensated LIVCR shown in Figure 6 and Figure 11, it can be seen that the disturbance perpendicular to the longitudinal axis is in opposite direction. There is some question whether this is due to the addition of the output choke coil or due to discrepancies in polarities recorded on the two respective tests. It is felt that the latter is the most likely explanation.

Performance tests show that the low input voltage converter-regulator operates at high efficiency throughout the 0.8 to 1.6 input voltage range with wide variations in load. The efficiency exceeds the 75% design goal at the rated 50 watts load for all input voltages in the specified range except the 1.6 volt input where the efficiency is 73%. The efficiency with a 1.6-volt input is lower at this point because the device operates at a much higher frequency and the percent conduction time of the voltage regulator is less, causing increased dissipation in the free wheeling diode.

By changing connections inside the unit to different output transformer taps, 75% efficiency at a 1.6 volt input and 50 watts load can be obtained. The voltage regulator provides a regulated 28-volt dc output over the above input voltage and 0 to 50 watt load ranges. Tests have shown that the current limiting overload protection circuit is suitable for charging batteries and powering dc motor loads. The overload protecting circuit limits the overload current to a preset level, operates for both slowly increasing overloads and sudden shorts, and recovers immediately once the overload has been reduced to a normal load. Since this low input voltage converter-regulator can condition the low variable voltage power to a higher regulated dc output voltage at high efficiency, it is suitable for conditioning the output from the new low voltage energy sources to provide a usable regulated voltage for powering future satellite electrical loads.

By utilizing the design approach developed during this program, low voltage converter-regulators having high performance and minimum external magnetic field disturbance are very promising for use on satellites carrying magnetometers for measuring the magnetic fields in space.

J.   RECOMMENDATIONS

Magnetic disturbance tests have shown that the external magnetic field
disturbance around the low input voltage converter-regulator can be
reduced to very low levels. Careful design procedures and successive
testing and modification of the device has resulted in successively lower
magnetic disturbance measurements. The magnetic disturbance remaining
in the unit is caused primarily by the high residual magnetic materials
used in the transistor cases and transistor leads and by the existence of
current loops that can cause disturbance when operating and that can also
perm the magnetic materials in the transistors. Transistors with non-
magnetic materials were not used in this model because of the difficulty
encountered in obtaining satisfactory devices at a reasonable cost.

It is recommended that transistors fabricated from non-magnetic materials
should be used in future devices having magnetic disturbance specifications.
It must be recognized that the price of these transistors may be high
because it will require special processing of units that are normally made
with magnetic materials. In this regard, it is also recommended that a
list of non-magnetic semi-conductors and their manufacturers be compiled
for use by technical personnel engaged in the design of electronic devices
to meet the magnetic disturbance requirements of spacecraft which carry
magnetometers.

The results of our magnetic disturbance tests have shown that current
loops, particularly those in the regulator section, cause disturbance when
operating. These tests have also shown that this disturbance can be
canceled by the placement of degaussing loops at appropriate positions in
the unit. The degree of cancellation that can be accomplished depends upon
the determination of the exact location, orientation, and magnitude of the
existing magnetic dipoles and the incorporation of a cancelling degaussing
coil in the proper location to accomplish effective cancellation. Successive

tests and modifications can produce more effective cancellation; however, it is difficult to insert the degaussing coil into the unit once the device has been fabricated. Therefore, it is recommended that all current paths should be carefully routed to minimize magnetic field disturbance. If current loops are unavoidable at certain locations, it is recommended that an equal and opposite loop be designed into the unit in sufficiently close to assure effective cancellation. This procedure is desirable since it is difficult to incorporate the loops later, and complete cancellation is difficult if the magnetic disturbance is caused by several distributed dipoles. A single degaussing loop cannot effectively cancel the disturbance caused by several distributed dipoles because the flux patterns from each dipole are centered about a different origin.

It is also recommended that the current through the degaussing loop be proportional to the current in the circuit loops that cause the original disturbance so that effective cancellation can be maintained over a wide input voltage and load operating range.

The low input voltage converter-regulator delivered under this contract weighed 5.16 pounds. This is 29% greater than the desired 4.0-pound weight. Part of the weight is due to the incorporation of the powdered permalloy choke core, which resulted in a slight increase in length and raised the unit weight from 4.8 pounds to 5.16 pounds. Since the weight of this device remains a paramount problem, it is recommended that further effort should be directed towards weight reduction. Future efforts should be directed towards the use of higher operating frequencies in the converter and in the voltage regulator to facilitate weight reduction. During this program, circuitry was developed that has increased the switching speed of the converter utilizing the low speed transistors (M. H. T. 2202 type). It is suggested that the use of higher speed diffused base transistors should be investigated for future higher frequency applications.

The converter-regulator fabricated under this contract was designed to meet performance, temperature, and magnetic field disturbance requirements. The coaxial construction used has resulted in other advantages (minimum input and primary inductance and excellent heat transfer). The work conducted on this device has proven the concept, and it is recommended that future effort be directed towards fabrication of a device to meet the environments encountered in a satellite (shock, vibration, altitude, etc.).

CALCULATION OF LIVCR (WITHOUT CHOKE) MAJOR
DIPOLE FOLLOWING 25 GAUSS EXPOSURE

The maximum magnetic disturbance caused by the LIVCR with a removed choke coil is presented in Figure 17. The disturbance as presented is the magnetic field directed collinear with the line connecting the geometric center of the LIVCR and the test point as the test probe is rotated around the device. The maximum total disturbance was along the longitudinal axis of the device and the source (dipole) appears to be off the geometric center. Recognizing this, the following calculations are made to determine the location and magnitude of this major dipole.

The magnetic field due to a simple dipole is given by the equation :

$$\overline{B} = \frac{\mu_o}{4\pi} \left[\frac{3M \cos\theta \; \overline{r}}{r^4} - \frac{\overline{M}}{r^3} \right]$$

Where
B = flux density in webers/meters^2
M = magnetic moment of dipole
r = distance from center of dipole to test point
θ = angle between $\overline{M}$ and $\overline{r}$
μ_o = permeability of air.

The disturbance at test point (A) is less than that at test point (B) and thus we can assume the dipole is located off center toward the regulator end of the LIVCR. The preceding equation reduces to the following form at these points.

$$\left| B_{\text{(A)}} \right| = 3 \times 10^{-9} = 10^{-7} \left[\frac{2M}{(R+y)^3} \right]$$

$$\left| B_{\text{(B)}} \right| = 14 \times 10^{-9} = 10^{-7} \left[\frac{2M}{(R-y)^3} \right]$$

Where R = 18 inches = 0.457 meters
y = off center displacement.
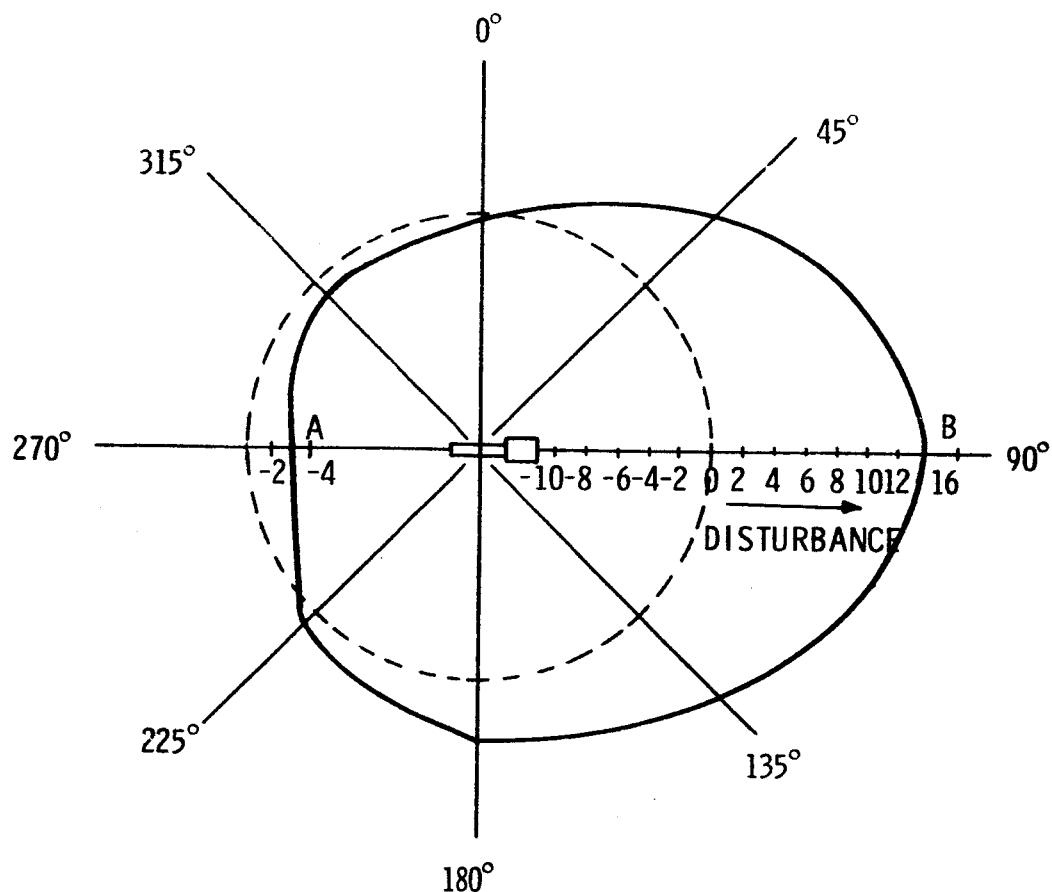
NOTE:

DISTURBANCE IN GAMMA

DISTURBANCE MEASURED ALONG RESPECTIVE RADIAL LINES

TEST POINT TO GEOMETRIC CENTER SEPARATION IS 18 INCHES

TESTS CONDUCTED 6-4-'65.

Figure 17 - LIVCR POST 25 GAUSS EXPOSURE MAGNETIC FIELD
(CHOKE REMOVED)

The equations will now be solved for y.

$$\frac{\left|B \; \textcircled{A}\right|}{\left|B \; \textcircled{B}\right|} = \frac{3}{14} = \frac{(R - y)^3}{(R + y)^3}$$

$$14 (R^3 - 3R^2y + 3Ry^2 - y^3) = 3 (R^3 + 3R^2y + 3Ry^2 + y^3)$$

$$y^3 - \left(\frac{11}{17}\right) 3Ry^2 + 3R^2y - \left(\frac{11}{17}\right) R^3 = 0$$

$$y^3 - 0.888 \, y^2 + 0.626 \, y - 0.062 = 0.$$

A cubic equation, $y^3 + py^2 + qy + m = 0$ may be reduced to the form

$$x^3 + ax + b = 0$$

Where $x = y + \frac{p}{3}$

$$a = \frac{1}{3} (3q - p^2)$$
$$b = \frac{1}{27} (2p^3 - 9pq + 27m).$$

Solving for

$$a = \frac{1}{3} (3q - p^2) = \frac{1}{3} [3 (0.626) - (0.888)^2] = 0.363$$

$$b = \frac{1}{27} [2p^3 - 9pq + 27m] = \frac{1}{27} [-1.4 + 5.0 - 1.68] = 0.071.$$

For the solution of the cubic equation let, -

$$A = \sqrt[3]{-\frac{b}{2} + \sqrt{\frac{b^2}{4} + \frac{a^3}{27}}} \quad , \quad B = \sqrt[3]{-\frac{b}{2} - \sqrt{\frac{b^2}{4} + \frac{a^3}{27}}}$$

and if $\frac{b^2}{4} + \frac{a^3}{27} > 0$, there will only be one real root with $x = A+B$.

$$\frac{b^2}{4} + \frac{a^3}{27} = \frac{(0.071)^2}{4} + \frac{(0.363)^3}{27} = 0.0031 \qquad 0.$$

$$A = \sqrt[3]{-0.0355 + 0.0555} = 0.271$$

$$B = \sqrt[3]{-0.0355 - 0.0555} = -0.450$$

$$x = 0.271 - 0.450 = -0.181$$

$$y = x - \frac{p}{3} = -0.181 - (\frac{-0.888}{3}) = +0.115 \text{ meters}$$
$$= 4.53 \text{ inches} .$$

Checking this value

$$0.214 = \frac{3}{14} = \frac{(R-y)^3}{(R+y)^3} = \frac{(0.457 - 0.115)^3}{(0.457 + 0.115)^3} = \frac{400}{1880} = 0.214 .$$

Thus the dipole is located 4.53 inches off the center and toward the regulator section. The magnitude may now be calculated

$$\left| B_{\text{Ⓐ}} \right| = 3 \times 10^{-9} = 10^{-7} \left[\frac{2M}{(0.457 + 0.115)^3} \right]$$

$$\left| M \right| = \frac{3 (0.572)^3 \, 10^{-2}}{2} = 2.80 \times 10^{-3} \text{ amp-meter}^2 .$$

APPENDIX B

CALCULATION OF THE MAGNITUDE AND GENERATED
FIELD OF COMPENSATING DIPOLES

The calculation of the magnitude of compensating dipoles M_1 and M_2 is based on LIVCR full load conditions. For this condition, the output current is 1.8 amperes.

Dipole M_1 is generated by a single turn of wire carrying load current and enclosing a circular area with a diameter of 1.75 inches (0.0444 meters). Therefore,

$$\left| M_1 \right| = N_1 I A_1 = (1)(1.8)(\frac{\pi}{4})(0.0444)^2 = 279 \times 10^{-5} \text{ amp-meters}^2.$$

Dipole M_2 is generated by 22 turns of wire carrying load current and enclosing a circular area with a mean diameter of 0.5 inches (0.0127 meters). Therefore

$$\left| M_2 \right| = N_2 I A_2 = (22)(1.8)(\frac{\pi}{4})(0.0127)^2 = 503 \times 10^{-5} \text{ amp-meters}^2.$$

Referring to Figure 8 for the dipole locations and to Figure 10 for the magnetic field test points, the following calculations are made to determine those fields due to the added dipoles. These calculations will be based on the equation for the disturbance at a point due to a simple dipole.

$$\bar{B} = \frac{\mu_o}{4\pi} \left(\frac{3M \cos \theta}{r^4} \bar{r} - \frac{1}{r^3} \bar{M} \right)$$

B = flux density in webers/meters^2

r = distance from center of dipole to test point

M = magnetic moment vector of dipole

θ = angle between $\bar{M}$ and $\bar{r}$

μ_o = permeability of air.

The disturbance calculations follow:

Test Point Ⓐ

EW Component

$$B_{M_1} = 10^{-7} \left[\frac{2(279 \times 10^{-5})}{(0.266)^3} \right] = \frac{558 \times 10^{-12}}{19 \times 10^{-3}} = +29.4 \text{ gamma W}$$

$$B_{M_2} = \frac{10^{-7} [3(503 \times 10^{-5})(0.07)]}{(0.370)^3} = \frac{105 \times 10^{-12}}{51.0 \times 10^{-3}} = +2.06 \text{ gamma W}$$

Total $\qquad$ 31.5 gamma W

NS Component

$$B_{M_1} = 0$$

$$B_{M_2} = \frac{-10^{-7}(503 \times 10^{-5})}{(0.370)^3} = \frac{-503 \times 10^{-12}}{51.0 \times 10^{-2}} = -9.9 \text{ gamma S}$$

Total $\qquad$ 9.9 gamma N

Test Point Ⓑ

EW Component

$$B_{M_1} = \frac{10^{-7}(279 \times 10^{-5})[-3(0.383)^2 + 1]}{(0.498)^3} = \frac{0.6(279 \times 10^{-12})}{124 \times 10^{-3}}$$

$$= \frac{168}{124} \times 10^{-9} = 1.35 \text{ gamma E}$$

-77-

$$B_{M_2} = \frac{10^{-7} (500) (3) (0.18) (0.18)}{(0.49)^3} = \frac{48.6 \times 10^{-12}}{118 \times 10^{-3}} = 0.41 \text{ gamma E}$$

Total   1.8 gamma E

NS Component

$$B_{M_1} = \frac{10^{-7} (279 \times 10^{-5}) (3) (0.383) (0.92)}{(0.498)^3} = \frac{295 \times 10^{-12}}{124 \times 10^{-3}} = 2.4 \text{ gamma N}$$

$$B_{M_2} = \frac{10^{-7} (500 \times 10^{-5}) [3 (0.98)^2 - 1]}{(0.49)^3} = \frac{940 \times 10^{-12}}{118 \times 10^{-3}} = 8.0 \text{ gamma S}$$

Total   5.6 gamma S

Test Point Ⓒ

EW Component

$$B_{M_1} = 1.35 \text{ gamma E}$$

$$B_{M_2} = \frac{10^{-12} (500) (3) (0.2) (0.2) (0.96)}{(0.466)^3} = \frac{7.5 \times 10^{-12}}{102 \times 10^{-3}} = 0.57 \text{ gamma E}$$

Total   1.9 gamma E

NS Component

$$B_{M_1} = 0$$

$$B_{M_2} = \frac{10^{-12} (500) [(3) (0.2) (0.2) (0.26) - 1]}{(0.466)^3} = \frac{500 \times 10^{-9}}{102} = 5 \text{ gamma N}$$

-78-

Vertical

$$B_{M_1} = 2.4 \text{ gamma Down}$$

$$B_{M_2} = \frac{10^{-12} (500) [(3)(0.2)(0.98)]}{(0.466)^3} = \frac{300 \times 10^{-12}}{102 \times 10^{-3}} = 3 \text{ gamma Up}$$

Total   0.6 gamma Up

Test Point Ⓓ

EW Component

$$B_{M_1} = 1.35 \text{ gamma E}$$

$$B_{M_2} = \frac{10^{-12} (500)(3)(0.2)(0.2) \times 10^{-5}}{(0.44)^3} = \frac{60 \times 10^{-12}}{86 \times 10^{-3}} = 0.7 \text{ W}$$

Total   0.7 gamma E

NS Component

$$B_{M_1} = 2.4 \text{ gamma S}$$

$$B_{M_2} = \frac{10^{-7} (500 \times 10^{-5}) [(3)(0.98)(0.98) - 1]}{(0.44)^3} = \frac{940 \times 10^{-12}}{86 \times 10^{-3}} = 11 \text{ gamma S}$$

Total   13.4 gamma S

Test Point Ⓔ

EW Component

$$B_{M_1} = 1.35 \text{ gamma E}$$

$$B_{M_2} = 0.57 \text{ gamma E}$$

Total 1.9 gamma E

-79-

NS Component

$$B_{M_1} = 0$$

$$B_{M_2} = 5 \text{ gamma S}$$

Total 5 gamma S

Vertical

$$B_{M_1} = 2.4 \text{ gamma Up}$$

$$B_{M_2} = 3 \quad \text{gamma Down}$$

Total 0.6 gamma Down

APPENDIX C

MAGNETIC DISTURBANCE MEASUREMENTS FROM TESTS CONDUCTED AT FREDERICKSBURG OBSERVATORY 24-25 JUNE 1965

TABLE I
INITIAL PERMANENT MAGNETIC FIELD MEASUREMENTS DUE TO LIVCR EXG2424N1X1

| Unit Orientation | | Sensor | | Disturbance (Gamma) | Comments |
Rotation Axis	Angle	Location From Unit Geometric Center	Orientation		
Vertical	0°	18" South	Vertical	0	
	90°			+1.4 Up	Very Noisy
	180°			+0.2 U	Ambient
	270°			0	
Vertical	315°			+1.0 U	Essentially Zero
North-South	0°-360°			0	
East-West	0°		Vertical	0	
	90°			+1.0 Down	
	180°			+0.6 D	
East-West	270°			+0.4 D	
Vertical	0°		North-South	+1.0 N	
	90°			+2.6 S	
	180°			+1.0 S	
Vertical	270°			0	
North-South	0°			+1.0 N	Noisy
	90°			0	
North-South	180°			+0.4 S	
East-West	270°			+0.2 N	
	0°		North-South	+1.0 N	
	90°			+1.0 N	
	180°			0.6 S	
East-West	270°		North-South	+0.6 N	
Vertical	0-360°		East-West	0	Essentially Zero
North-South	0-360°			0	Essentially Zero
East-West	0-360°	18" South	East-West	0	Essentially Zero

TABLE II

PERMANENT MAGNETIC FIELD MEASUREMENTS AFTER 25 GAUSS EXPOSURE

Unit Orientation Rotation Axis	Angle	Location From Unit Geometric Center	Sensor Orientation	Disturbance (Gamma)	Comments
Vertical	0°-360°	18" South	Vertical	~0.5	Noisy
North-South	0°		Vertical	0	
North-South	90°			+2.4 U	
	180°			+0.6 D	
	270°			+4.0 D	
East-West	0°-360°			~0	Essentially Zero
Vertical	0°		Vertical	+4 N	
	90°		North-South	+7.2 N	
	180°			+4 N	
Vertical	270°			+12.0 S	
North-South	0°-360°		North-South	+4 N	Essentially No Change With Rotation
East-West	0°-360°			+4 N	Essentially No Change With Rotation
Vertical	0°		East-West	+3.4 E	
	45°-135°			+1.0 E	
	180°			+0.6 W	
	225°			+3.8 W	
	270°			+0.6 W	
Vertical	315°			+5.4 E	
North-South	0°-360°			+3.4 E	
East-West	0°-360°	18" South	East-West	+3.4 E	Essentially No Change With Rotation
Vertical	0°-360°	36" South	North-South	<±0.8	Noisy
North-South	0°-360°	36" South	North-South	~0	Essentially Zero

TABLE III

PERMANENT MAGNETIC FIELD MEASUREMENTS AFTER DEPERMING

Unit Orientation		Sensor		Disturbance (Gamma)	Comments
Rotation Axis	Angle	Location From Unit Geometric Center	Orientation		
Vertical	0°-360°	18" South	Vertical	~0	Essentially Zero
North-South	0°-360°		Vertical	~0	Essentially Zero
East-West	0°-360°		Vertical	~0	Essentially Zero
Vertical	0°		North-South	+0.5 N	
	90°			+1.1 S	Low Signal to Noise
	180°			+1.1 S	
Vertical	270°			+0.5 N	
North-South	0°-360°		North-South	~0	
East-West	0°-360°	18" South	East-West	~0	Essentially Zero for All Rotations

TABLE IV

INDUCED MAGNETIC FIELD MEASUREMENTS WITH 26,000 GAUSS PRIMARY FIELD

Essentially no disturbance was noted in the horizontal plane due to the introduction of LIVCR EXG2424N1X1 into the 26,000 gamma vertical field test area.

TABLE V

STRAY MAGNETIC FIELD DUE TO CIRCULATORY CURRENTS MEASUREMENTS (POWER ON/POWER OFF)

| Unit Orientation | | Sensor | | Measured | Selected Points for |
Rotation Axis	Angle	Location From Unit Geometric Center	Orientation	Disturbance (Gamma)	Comparing Disturbance with No Compensation In.
East-West	0°	18" South	Vertical	0	+2.0 U
	90°		↕	+2.4 U	+1.6 D
	180°		Vertical	+1.6 D	+3.2 N
	270°			+1.4 D	+13.0
	0°		North-South	+0.4 N	+2.8 E
	90°			+1.4 S	+4.0 W
	180°		North-South	+0.4 N	
	270°			+6.0 S	+1.2 D
	0°		East-West	+5.6 E	
	90°			+1.6 E	+2.6 S
	180°		East-West	+4.6 W	
	270°			+1.2 E	+23.0 E
	0°		Vertical	+6.4 U	+1.4 E
	90°			+11 U	
	180°		Vertical	+0.6 U	
	270°	18" South		-10 D	
	0°	18" West	North-South	+11 N	
	90°			0	
	180°		North-South	+10.5 S	
	270°			+1 N	
	0°		East-West	+6.4 W	
	90°			+8.6 W	
	180°		East-West	+9.0 W	
East-West	270°	18" West	East-West	+7.0 W	
	0°–360°	36" West	East-West	<0.5 γ	

Other measurements taken at 36" rejection indicated disturbances less than ±0.5γ but were buried in the noise.

APPENDIX D

CALCULATION OF THE MAGNETIC DISTURBANCE DUE TO DIPOLES REPRESENTING THE UNCOMPENSATED LIVCR

Dipole M_3 is assumed to be located in the same position as compensating dipole M_2 (Figure 8) and to have the same magnitude, but being opposite in direction. Another dipole M_4 is assumed to be located in the same posititition as compensating dipole M_1, but directed 45° North from the longitudinal axis with a magnitude of 300 amp-meters^2 (see Figure 8).

The disturbance from these two dipoles is presented below using the approach analogous to that of Appendix B. Refer to Figure 10 for test points.

Test Point(A)

NS Component $\qquad$ B_{M_3} = 9.9 gamma S

$$B_{M_4} = \frac{10^{-12} (300) (0.7)}{19 \times 10^{-3}} \qquad = \quad \underline{11 \quad \text{gamma N}}$$

Total $\qquad$ 1.1 gamma N

EW Component $\qquad$ B_{M_3} = 2 gamma E

$$B_{M_A} = 10^{-12} \frac{[-3 (300) (0.7) + 300 (0.7)]}{19 \times 10^{-3}} = 22 \text{ gamma E}$$

Total $\qquad$ 24 gamma E

Test Point Ⓑ

EW Component $\qquad B_{M_3} = 0.4$ gamma W

$$B_{M_4} = \frac{10^{-12}\left[3\,(300)\,(0.92)\,(0.383) - 300\,(0.7)\right]}{124 \times 10^{-3}} = .85 \text{ gamma E}$$

Total $\quad .45$ gamma E

NS Component

$$B_{M_3} = 8.0 \text{ gamma N}$$

$$B_{M_4} = \frac{10^{-12}\left[3(300)\,(0.92)\,(0.92) - 300\,(0.7)\right]}{124 \times 10^{-3}} = 4.4 \text{ gamma S}$$

Total $\quad 3.6$ gamma N

Test Point Ⓒ

EW Component

$$B_{M_3} = 0.6 \text{ gamma W}$$

$$B_{M_4} = \frac{10^{-12}\left[3\,(300)\,(0.383)\,(0.383) - 300\,(0.7)\right]}{124 \times 10^{-3}} = 0.6 \text{ gamma W}$$

Total $\quad 1.2$ gamma W

NS Component

$$B_{M_3} = 5 \text{ gamma S}$$

$$B_{M_4} = \frac{10^{-12} (0.7)(300)}{124 \times 10^{-3}} = 1.7 \text{ gamma N}$$

$$\text{Total} \quad 3.3 \text{ gamma S}$$

Vertical Component

$$B_{M_3} = 3 \text{ gamma Down}$$

$$B_{M_4} = \frac{10^{-12} [3(300)(0.92)(0.383)]}{124 \times 10^{-3}} = 2.6 \text{ gamma Up}$$

$$\text{Total} \quad 0.4 \text{ Down}$$

Test Point Ⓓ

EW Component

$$B_{M_3} = 0.7 \text{ gamma E}$$

$$B_{M_4} = \frac{10^{-12} (3(300)(0.2)(0.383) - (0.7)(300)]}{124 \times 10^{-3}} = 1.1 \text{ W}$$

$$\text{Total} \quad 0.4 \text{ gamma W}$$

NS Component

$$B_{M_3} = 11 \text{ gamma N}$$

$$B_{M_4} = \frac{10^{-12}\,[3\,(300)\,(0.2)\,(0.92) - (0.7)\,(300)]}{124 \times 10^{-3}} = \frac{0.35\ \text{N}}{\text{Total} \quad 11.3 \text{ gamma N}}$$

Test Point Ⓔ

EW Component

$$B_{M_3} = 0.6 \text{ gamma W}$$

$$B_{M_4} = \underline{\quad 0.6 \text{ gamma W} \quad}$$

Total   1.2 gamma W

NS Component

$$B_{M_3} = 5 \text{ gamma N}$$

$$B_{M_4} = \underline{\quad 1.7 \text{ gamma N} \quad}$$

Total   6.7 gamma North

Vertical Component

$$B_{M_3} = 3 \text{ gamma Up}$$

$$B_{M_4} = \underline{\quad 2.6 \text{ gamma Down} \quad}$$

Total   0.4 gamma Up

APPENDIX E*

THE CONSTANT-FIELD COIL HOUSE

AT THE

FREDERICKSBURG MAGNETIC OBSERVATORY

J. H. Nelson, R. E. Gebhardt, J. L. Bottum

Geophysics Division, U. S. Coast and Geodetic Survey

Abstract. When plans were made for the construction and operation of the Fredericksburg Magnetic Observatory and Laboratory, they included the installation of a set of large coils with which it would be possible to duplicate the geomagnetic field at any place on the earth. For this purpose, two sets of coils were constructed, having a common center -- one set for control of the Z field, the other with its axis horizontal and approximately in the mean magnetic meridian. Each coil form has a main, or primary, winding and an auxiliary, or secondary, winding. A helmholtz coil was later installed with its axis in the magnetic east-west direction.

Automatic control circuits are provided for maintaining steady currents in the primary windings of the H and Z coils, constant to about ± 5 microamp, which is equivalent to about 3 parts in 10^6.

Other automatic controls provide currents in the east-west (D) coils, and in the secondary windings of the H and Z coils, that vary in amplitude and polarity so as to produce component fields that just neutralize the variations of the earth's field, thus maintaining within the coils a constant field.

---

* This appendix presents only the Abstract of the subject report. The report was published by the U. S. Department of Commerce, Coast and Geodetic Survey, Washington 25, D.C.

APPENDIX F

PERFORMANCE DATA FOR LIVCR EXG2424N1X1

UNITS TESTED:

One EXG 2424N1X1 Coaxial Low Input Voltage Converter. Manufactured by Honeywell Ordnance Tech Lab.

OBJECT OF TEST:

At input voltages of 0.8, 1.0, 1.2, 1.4, 1.6 VDC measure input voltage, input current, output current, output voltage and output ripple voltage for the output power range of 5 to 50 watts. Obtain the above data at room ambient, +160°F and +14°F.

At room temperature and input voltages of 0.8 and 1.6 VDC obtain input current, output current, and output voltage for the load range from 50 watts to short circuit.

DOCUMENTATION:

The data is presented in Tables 1 to 4 and in Graphs 1 to 3.

TABLE 1 - TEST AT ROOM TEMPERATURE

Load Range W.	I-N-P-U-T E=V.	I-N-P-U-T I=A	I-N-P-U-T W	O-U-T-P-U-T E=V	O-U-T-P-U-T I=A	O-U-T-P-U-T W	R-I-P-P-L-E MV	R-I-P-P-L-E MV*	Efficiency (± 1.5% Accuracy) %
5	0.8	11.4	9.16	28.2	0.180	5.1	12	+ 2	55.5
10	"	16.1	12.9	28.2	0.359	10.1	12	+ 2	78.3
20	"	32.0	25.6	28.1	0.710	20.0	11	+ 3	78.3
35	"	56.5	45.2	28.07	1.25	35.1	8	+ 4	77.7
50	"	81.4	65.1	27.9	1.78	49.7	6	+ 6	76.4
5	1.0	13.0	13.0	28.60	0.181	5.17	27	+ 2	39.8
10	"	15.5	15.5	28.38	0.359	10.4	27	+ 2	67.3
20	"	24.8	24.8	28.30	0.709	20.0	28	+ 3	80.8
35	"	44.0	44	28.25	1.24	35.0	28	+ 3	79.5
50	"	65.0	65	28.10	1.78	50.0	28	+ 3	77.0
5	1.2	12.0	14.4	28.60	0.181	5.17	30	+ 2	35.9
10	"	15.7	18.8	28.40	0.360	10.4	36	+ 3	55.3
20	"	21.5	25.8	28.30	0.720	20.4	37	+ 5	65.7
35	"	36.8	44.2	28.30	1.24	35.0	40	±10	79.2
50	"	54.4	65.5	28.10	1.78	50.0	40	±10	77.0
5	1.4	11.2	15.7	28.50	0.181	5.15	34	+ 2	32.8
10	"	17.2	24.1	28.40	0.360	10.2	40	+ 2	42.4
20	"	20.2	28.3	28.30	0.720	20.4	41	+ 2	72.2
35	"	32.1	45.0	28.20	1.24	35.0	45	+ 3	77.7
50	"	47.5	66.5	28.10	1.78	50.0	47	+	75.3
5	1.6	11.5	18.4	28.25	0.181	5.1	35	+ 0	27.7
10	"	17.5	28.0	28.20	0.360	10.1	43	+ 0	36
20	"	22.5	36.0	28.18	0.720	20.6	50	+ 1	57.3
35	"	28.8	46.1	28.18	1.24	34.9	50	+ 1	75.7
50	"	42.0	67.2	27.75	1.78	49.5	54	+	73.5

*Transient spike reading

-91-

TABLE 2 - OVERLOAD TEST   ROOM TEMPERATURE

Inp. Range	I - N - P - U - T		O - U - T - P - U - T	
	E = V	I = A	E = V	I = A
0.8v	0.8	73.0	28.0	1.625
	"	89.0	27.6	1.920
	"	83.4	27.0	1.930
	"	79.5	26.0	1.875
	"	46.8	14.0	2.18
	"	9.0	0.05	2.42
1.6v	1.6	32.5	28.00	1.425
	"	50.5	27.6	2.16
	"	54.3	27.0	2.37
	"	53.1	26.0	2.40
	"	32.0	14.0	2.58
	"	10.0	0.05	2.85

TABLE 3 - TEST AT 160°F

STABILIZATION TIME - 3 HOURS

Load Range W.	I - N - P - U - T			O - U - T - P - U - T			R-I-P-P-L-E		Efficiency (±1.5% Accuracy)
	E = V	I = A	W	E = V	I = A	W	MV	MV*	%
5	0.8	13.5	10.8	28.45	0.180	5.12	15	+ 15	47.4
10	"	16.7	13.35	28.42	0.360	10.2	15	+ 15	75.5
20	"	31.5	25.2	28.40	0.710	20.2	12	+ 20	80.0
35	"	58.0	46.4	28.39	1.25	35.4	13	+ 20	76.1
50	"	87.3	69.8	28.20	1.78	50.2	12	+ 20	72.0
5	1.0	15.5	15.5	28.81	0.181	5.22	24	+ 20	33.7
10	"	16.8	16.8	28.60	0.359	10.27	30	+ 25	61.2
20	"	25.6	25.6	28.60	0.709	20.30	27	+ 27	79.3
35	"	46.0	46.0	28.55	1.24	35.3	21	+ 25	76.8
50	"	67.8	67.8	28.31	1.78	50.7	25	+ 25	74.8
5	1.2	16.7	20.0	28.80	0.182	5.25	28	+ 15	26.2
10	"	19.4	23.3	28.72	0.359	10.3	31	+ 20	44.3
20	"	22.5	27.0	28.60	0.720	20.6	35	+ 25	76.3
35	"	34.0	46.8	28.55	1.24	35.3	37	+ 30	75.4
50	"	57.0	68.4	28.39	1.78	50.5	39	+ 35	73.8
5	1.4	17.7	24.8	28.70	0.182	5.22	30	+ 20	21.1
10	"	22.0	30.8	28.60	0.359	10.25	39	+ 40	33.3
20	"	20.8	29.1	28.58	0.720	20.6	43	+ 45	70.8
35	"	34.5	48.4	28.50	1.23	35.0	44	+ 45	72.3
50	"	50.4	70.6	28.30	1.78	50.5	47	+ 50	71.7
5	1.6	19.1	30.6	28.60	0.181	5.18	33	+ 23	16.9
10	"	24.5	39.2	28.58	0.359	10.0	42	+ 28	25.6
20	"	30.0	48.0	28.42	0.719	20.4	50	+ 30	42.5
35	"	31.9	51.1	28.41	1.24	35.2	51	+ 40	69.0
50	"	46.0	73.6	28.19	1.78	50.2	56	+ 45	68.3

*Transient spike reading

TABLE 4 – TEST AT 14°F

STABILIZATION TIME 1.5 HOURS

Load Range W	I-N-P-U-T E=V	I-N-P-U-T I=A	I-N-P-U-T W	O-U-T-P-U-T E=V	O-U-T-P-U-T I=A	O-U-T-P-U-T W	R-I-P-P-L-E MV	R-I-P-P-L-E MV*	Efficiency (±1.5% Accuracy) %
5	0.8	9.0	7.2	28.09	0.180	5.05	14	+ 5	70.0
10	"	16.1	12.9	26.05	0.359	10.08	15	+ 8	78.2
20	"	31.0	24.8	28.00	0.710	19.9	15	+ 10	80.3
35	"	54.0	43.3	28.00	1.25	35.0	16	+ 20	80.8
50	"	80.0	64.0	27.9	1.78	49.7	14	+ 25	77.8
5	1.0	11.0	11.0	28.5	0.181	5.16	35	+ 15	46.8
10	"	13.5	13.5	28.25	0.359	10.12	35	+ 15	75.2
20	"	?.0	25.0	28.22	0.709	20.0	37	+ 20	80.0
35	"	42.5	42.5	28.2	1.24	35.00	38	+ 20	82.4
50	"	62.4	62.4	28.0	1.78	49.8	39	+ 25	79.8
5	1.2	11.0	13.4	28.5	0.180	5.13	41	+ 10	38.3
10	"	14.5	17.4	28.35	0.359	10.15	46	+ 10	58.3
20	"	21.4	25.7	28.20	0.719	20.15	47	+ 10	78.4
35	"	35.8	43.0	28.20	1.24	35.00	49	+ 20	81.4
50	"	51.7	62	28.0	1.78	49.80	50	+ 20	80.4
5	1.4								
10	"								
20	"								
35	"								
50									
5	1.6	11.2	17.9	28.21	0.180	5.07	43	+ 10	28.3
10	"	16.2	25.9	28.2	0.360	10.15	55	+ 15	39.2
20	"	13.6	29.9	28.1	0.720	20.2	61	+ 20	67.6
35	"	27.8	44.5	28.0	1.24	34.8	68	+ 25	78.2
50	"	39.1	62.7	27.9	1.78	49.7	72	+ 28	78.0

*Transient spike reading

APPENDIX G

ENGINEERING PARTS LIST

EXG 2424N1X1

CONVERTER REGULATOR

Part No.	Part Name	Rating	Designation	Quantity
3. 3K ohm	Resistor	0. 1 watt	R1, 9	2
150			R2	1
1K		1 watt	R3	1
4. 3K		0. 1 watt	R4	1
68K			R5, 8, 12	3
5K	Potentiometer	1/4 watt	R6, 18	2
47K	Resistor	0. 1 watt	R7, 16	2
10K			R10, 13, 14	3
680			R15	1
1K		0. 1 watt	R18, 21, 22	3
75		1 watt	R19	1
4. 7K		0. 1 watt	R20	1
22K			R23	1
2. 2K		2 watt	R26	1
5K		2 watt	R28	1
. 025		Nichrome Wire	R29	1
33K		0. 1 watt	R30	1
10 MFD	Capacitor	35 VDC	C1, 2, 6, 7	4

Part No.	Part Name	Rating	Designation	Quantity
0. 1 MFD	Capacitor	35 VDC	C3, 4	2
.0001 MFD		35 VDC	C5	1
100 MFD		10 VDC	C8	1
10 MFD		70 VDC	C10	7
0. 01 MFD		35 VDC	C13, 15	2
220 MFD		40 VDC	C14	6
150 MFD		20 VDC	C16	1
			CR1, 2, 3, 4, 5, 6, 30, 31	8
IN3730	Diode	750 M. A.	CR7, 15, 17, 20	
IN4003	Diode	750 M. A.	21, 28, 29, 32	7
IN645	Diode	400 M. A.	CR8, 9, 10, 11, 12, 13	6
IN823	Zener Diode	6V	CR14, 16, 22	3
HGR-10-150	Diode	10A	CR18, 19, 26	3
IN643A	Diode	200 MW	CR23, 25, 27	3
IN3685B	Zener Diode	18V	CR24	1
MHT 2202	Transistor		Q1, 2, 3, 4	4
2N2000			Q5	1
2N489			Q6	1
2N2223			Q7-8	1
2N3019			Q9	1
2N718			Q10, 12, 15, 16	4

Part No.	Part Name	Rating	Designation	Quantity
2N720			Q11	1
2N2469			Q13	1
2N2833	Transistor		Q14	1
	Feedback Transformer		T1	1
	Pulse Transformer		T2	1
	Decoupling Transformer		T3, 4	2
	Power Transformer		T5	1
	Current Transformer		T6	1
	Timing Reactor		L1	1
	Interbase Choke		L2	1
	Choke Coil		L3	1

BLANK